A Meshless Approach to Spectral Wave Modeling

Adrean Webb

The University of Tokyo
Graduate School of Frontier Sciences

August 7, 2017

In Collaboration with: Natasha Flyer (NCAR), Baylor Fox-Kemper (Brown University)

Outline

1. Scientific background
2. Coupled wave component
3. Overview of meshless approach
4. Kinematic prototype
5. Discussion

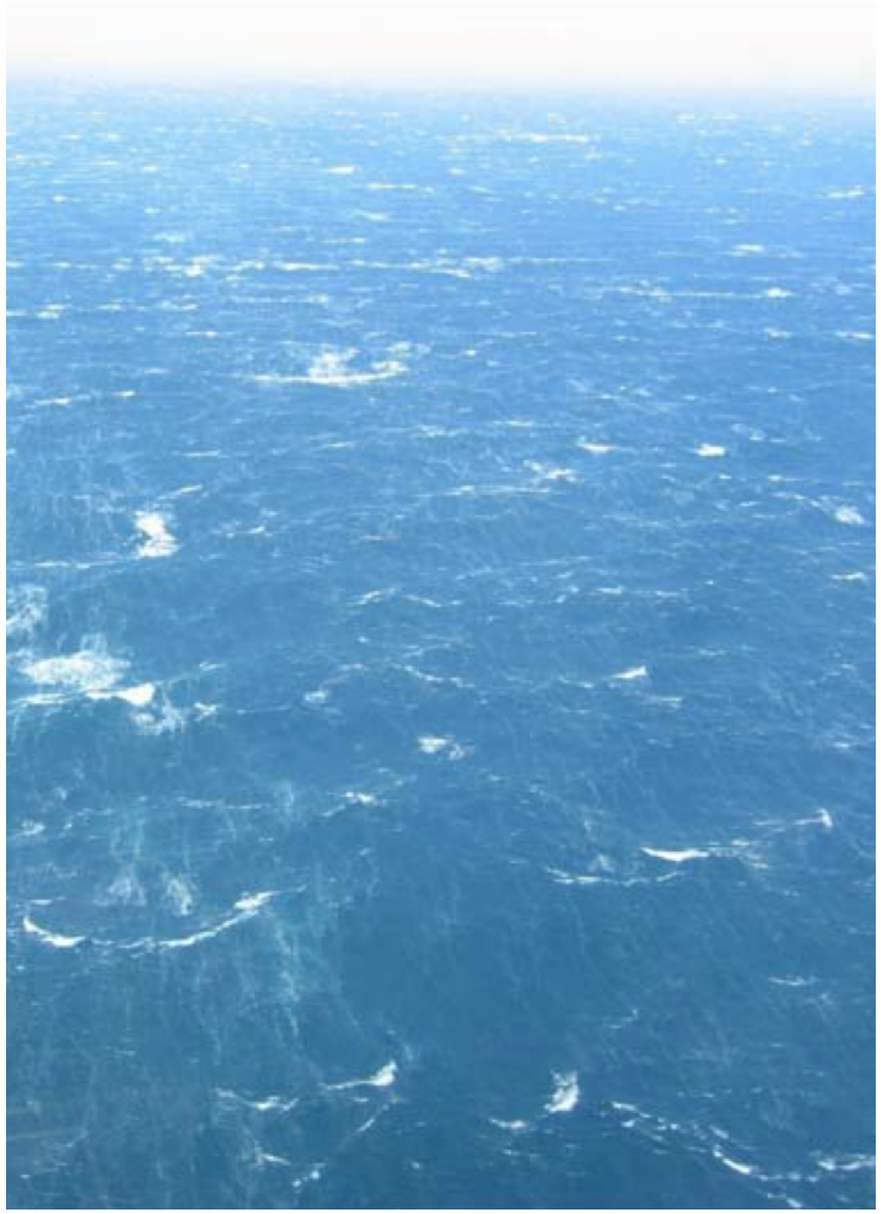

Scales of interest

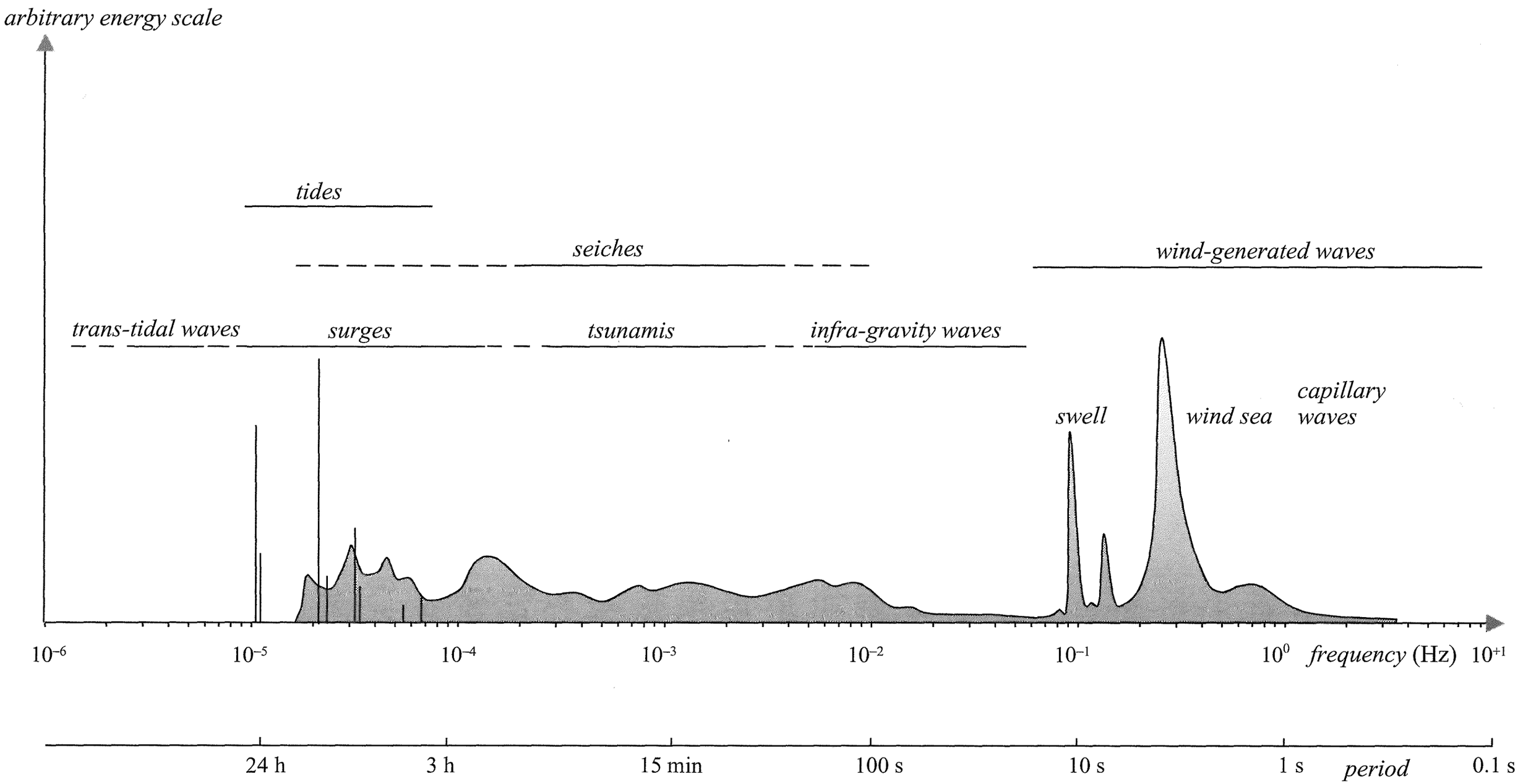

Figure: Illustration of wave spectra from different types of ocean surface waves (Holthuijsen, 2007).

Spectral wave model approach

The statistical properties on intermediate scales are assumed to vary smoothly with location and the generation, propagation, and evolution of wave spectra are modeled deterministically.

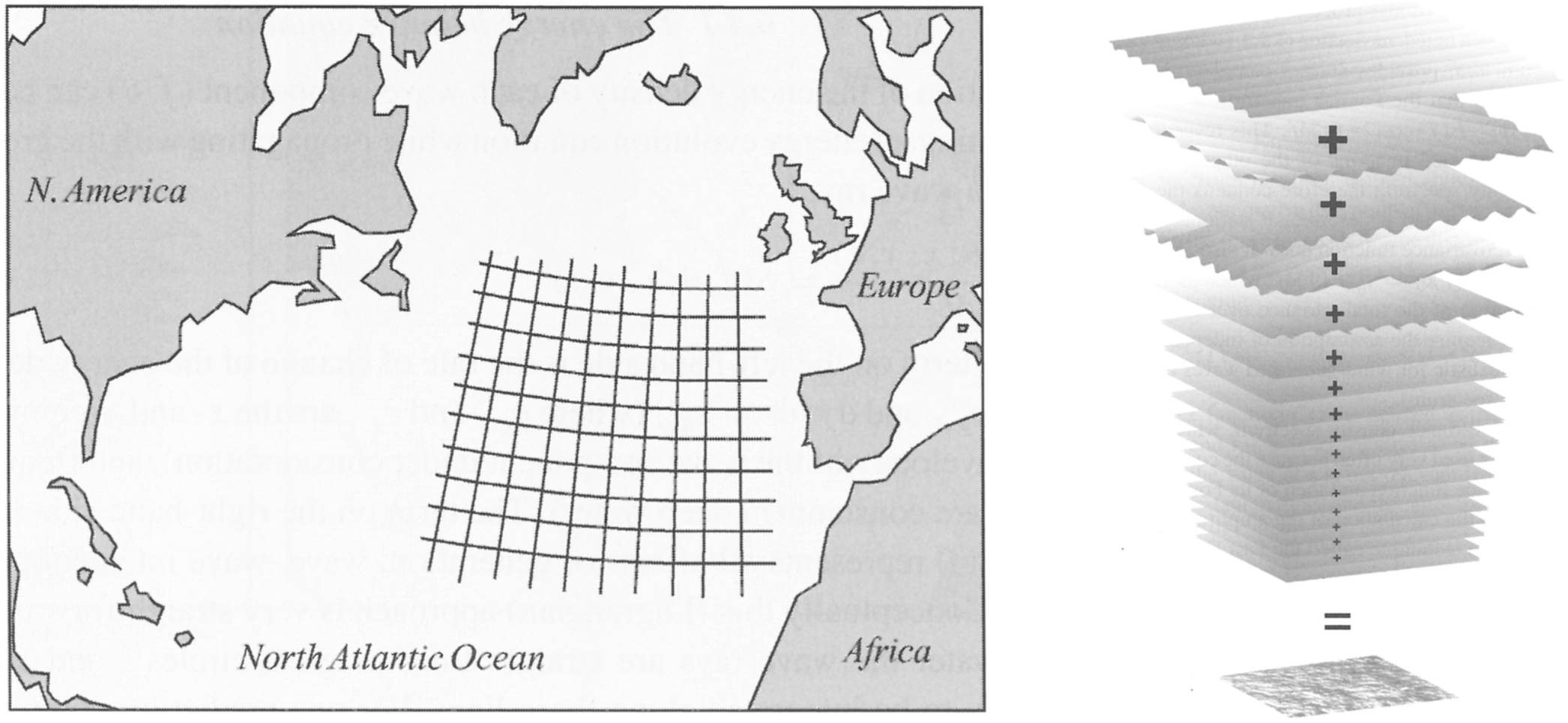

Figure: The random sea of each gridded region in (a) is Fourier decomposed in (b). The statistical differences between neighboring gridded regions are assumed to be small enough such that advection and evolution of wave energy can be modeled by a PDE (Holthuijsen, 2007)

Sample spectral model output

Figure: Global surface Stokes drift on a 1 deg lat x 1.25 deg lon grid.

Wave action balance equation

The *wave action balance equation* can be derived on a coupled slab ($\vec{x}, \vec{k} \in \mathbb{R}^2$) from the *governing linear wave equations* and is given by

$$\partial_t \mathcal{W} + \nabla_{\vec{k}} \Omega \cdot \nabla_{\vec{x}} \mathcal{W} - \nabla_{\vec{x}} \Omega \cdot \nabla_{\vec{k}} \mathcal{W} = \text{Sources}$$

where

- $\sigma(\vec{x}, \vec{k}) = \left\{ g|\vec{k}| \tanh\left[|\vec{k}| H(\vec{x})\right] \right\}^{1/2}$ is the *intermediate-water dispersion relation*
- $\Omega(\vec{x}, \vec{k}) = \vec{U}(\vec{x}) \cdot \vec{k} + \sigma(\vec{x}, \vec{k})$ is the *Doppler-shifted dispersion relation*
- $\mathcal{W}(\vec{x}, \vec{k}, t) = \mathrm{g}\, \mathcal{S}_{\vec{k}}(\vec{k}; \vec{x}, t) \,/\, \sigma(\vec{x}, \vec{k})$ is the *spectral adiabatic invariant*
- "Sources" encompass the non-kinematic physics of the waves (generation, dissipation, nonlinear interactions, etc.)

Wave action balance equation

The *wave action balance equation* can be derived on a coupled slab ($\vec{x}, \vec{k} \in \mathbb{R}^2$) from the *governing linear wave equations* and is given by

Spatial transport

$$\partial_t \mathcal{W} + \nabla_{\vec{k}} \Omega \cdot \nabla_{\vec{x}} \mathcal{W} - \nabla_{\vec{x}} \Omega \cdot \nabla_{\vec{k}} \mathcal{W} = \text{Sources}$$

Spatial changes

where

- $\sigma(\vec{x}, \vec{k}) = \left\{ g|\vec{k}| \tanh\left[|\vec{k}| H(\vec{x})\right] \right\}^{1/2}$ is the *intermediate-water dispersion relation*
- $\Omega(\vec{x}, \vec{k}) = \vec{U}(\vec{x}) \cdot \vec{k} + \sigma(\vec{x}, \vec{k})$ is the *Doppler-shifted dispersion relation*
- $\mathcal{W}(\vec{x}, \vec{k}, t) = \mathrm{g}\, \mathcal{S}_{\vec{k}}(\vec{k}; \vec{x}, t) \,/\, \sigma(\vec{x}, \vec{k})$ is the *spectral adiabatic invariant*
- "Sources" encompass the non-kinematic physics of the waves (generation, dissipation, nonlinear interactions, etc.)

Wave action balance equation

The *wave action balance equation* can be derived on a coupled slab ($\vec{x}, \vec{k} \in \mathbb{R}^2$) from the *governing linear wave equations* and is given by

Spectral transport

$$\partial_t \mathcal{W} + \nabla_{\vec{k}} \Omega \cdot \nabla_{\vec{x}} \mathcal{W} - \nabla_{\vec{x}} \Omega \cdot \nabla_{\vec{k}} \mathcal{W} = \text{Sources}$$

Spectral changes

where

- $\sigma(\vec{x}, \vec{k}) = \left\{ g|\vec{k}| \tanh\left[|\vec{k}| H(\vec{x})\right] \right\}^{1/2}$ is the *intermediate-water dispersion relation*
- $\Omega(\vec{x}, \vec{k}) = \vec{U}(\vec{x}) \cdot \vec{k} + \sigma(\vec{x}, \vec{k})$ is the *Doppler-shifted dispersion relation*
- $\mathcal{W}(\vec{x}, \vec{k}, t) = \mathrm{g}\, \mathcal{S}_{\vec{k}}(\vec{k}; \vec{x}, t) \,/\, \sigma(\vec{x}, \vec{k})$ is the *spectral adiabatic invariant*
- "Sources" encompass the non-kinematic physics of the waves (generation, dissipation, nonlinear interactions, etc.)

Outline

1. Scientific background
2. Coupled wave component
3. Overview of meshless approach
4. Kinematic prototype
5. Discussion

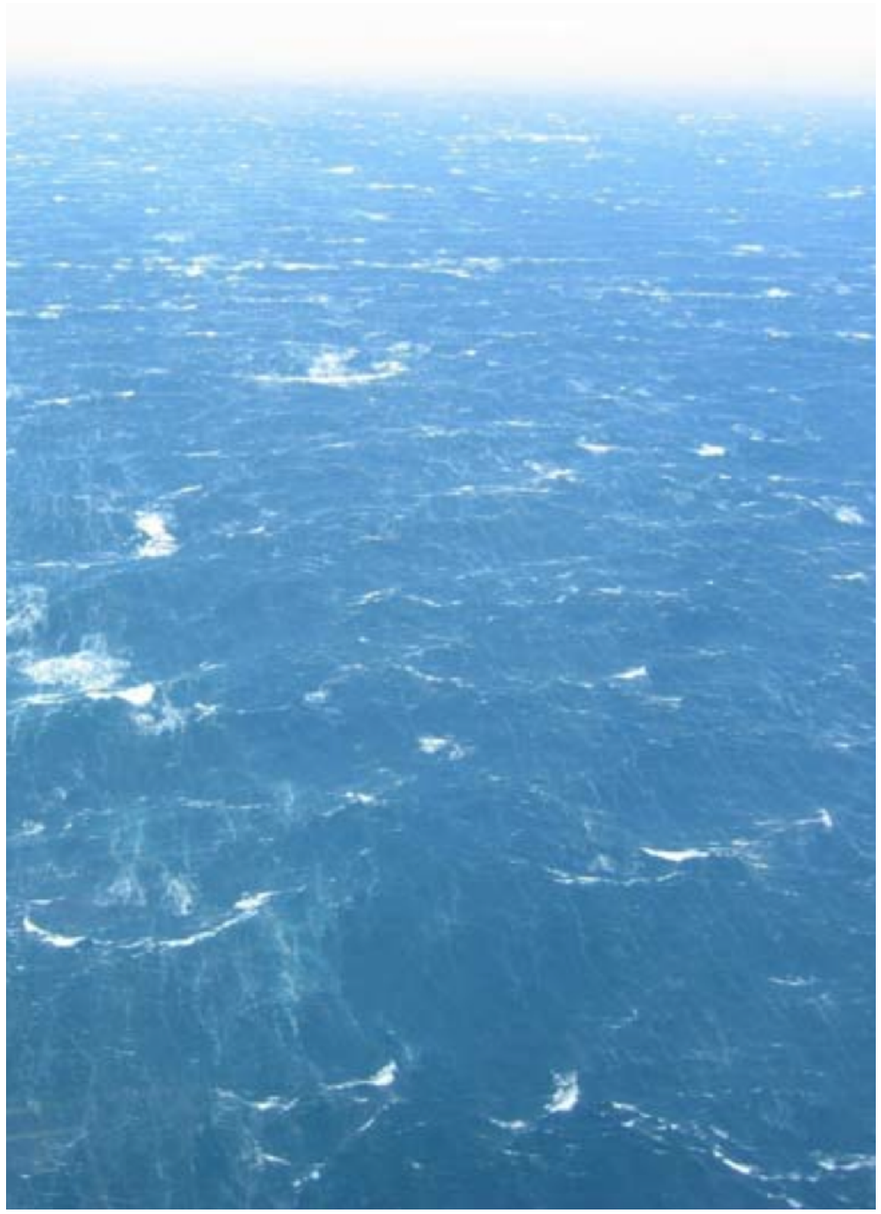

Scientific Motivation

There is a persistent, shallow mixed layer bias in the Southern Ocean in global climate models (GCMs): Langmuir turbulence missing??

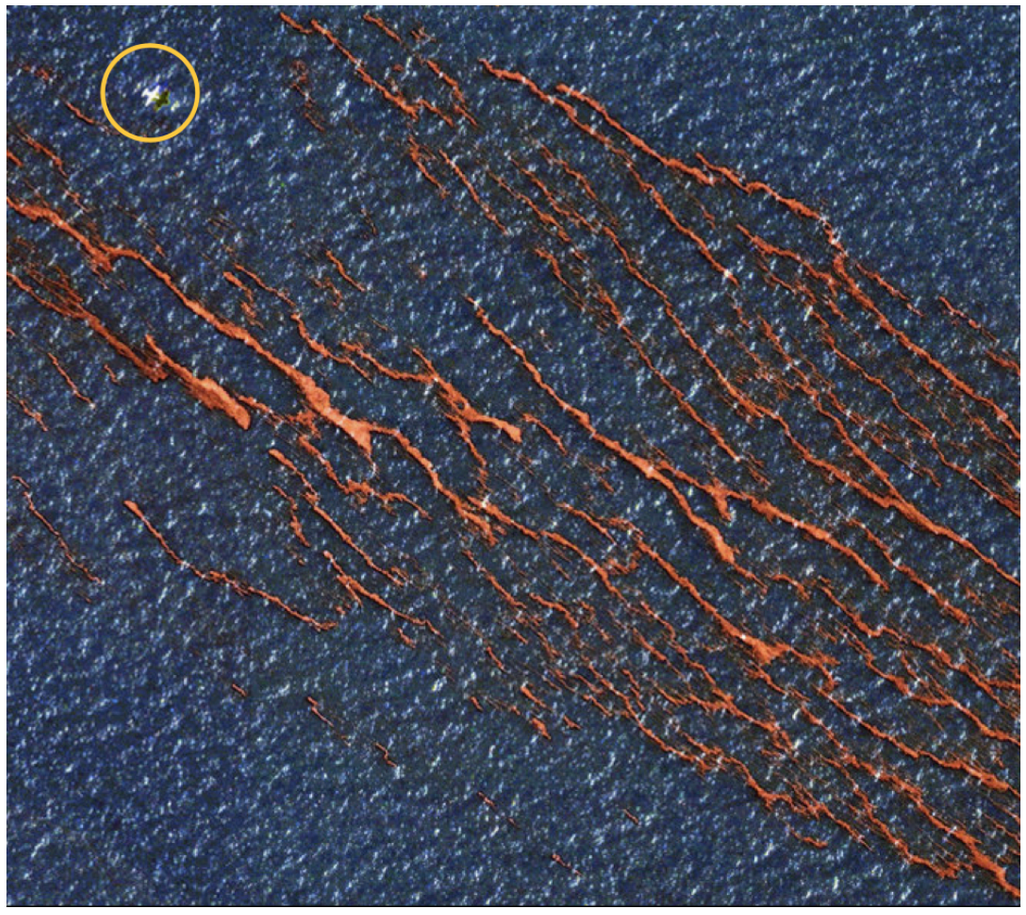

Figure: Satellite observations of Langmuir turbulence after the Deepwater Horizon oil spill (Quickbird)

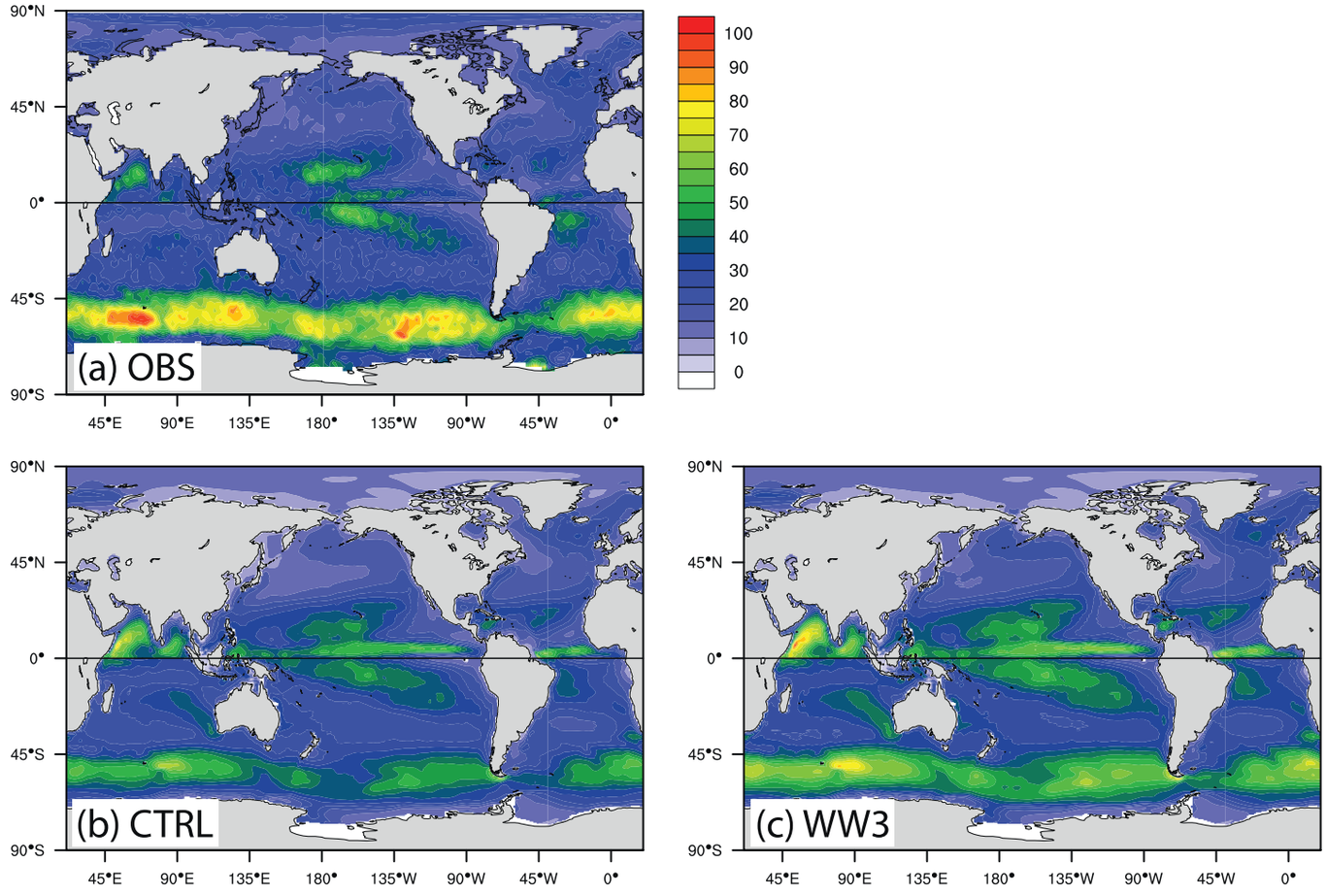

Figure: Mixed layer bias is reduced in NCAR CESM model runs (Li, Fox-Kemper, Breivik, & Webb, 2017).

Other studies: Belcher et al. 2012; D'Asaro et al., 2014; Fan & Griffies, 2014

NCAR CESM now includes a prognostic wave field

Modified NOAA WAVEWATCH III has been coupled to NCAR CESM (Craig, Li, Vertenstein, Webb)

Third-generation model:

- Creates and evolves wave spectra in a coupled spatial-spectral domain
- Uses structured grids (lat-lon, polar)
- Includes extensive physics and parameterizations

Drawbacks for climate use:

- Computational expensive
  - 4D problem in time with 6-50 x 10^6 unknowns and nonlinear source terms
- Spatial and spectral singularities at the poles
  - Difficult to model polar-ice-free climate scenarios

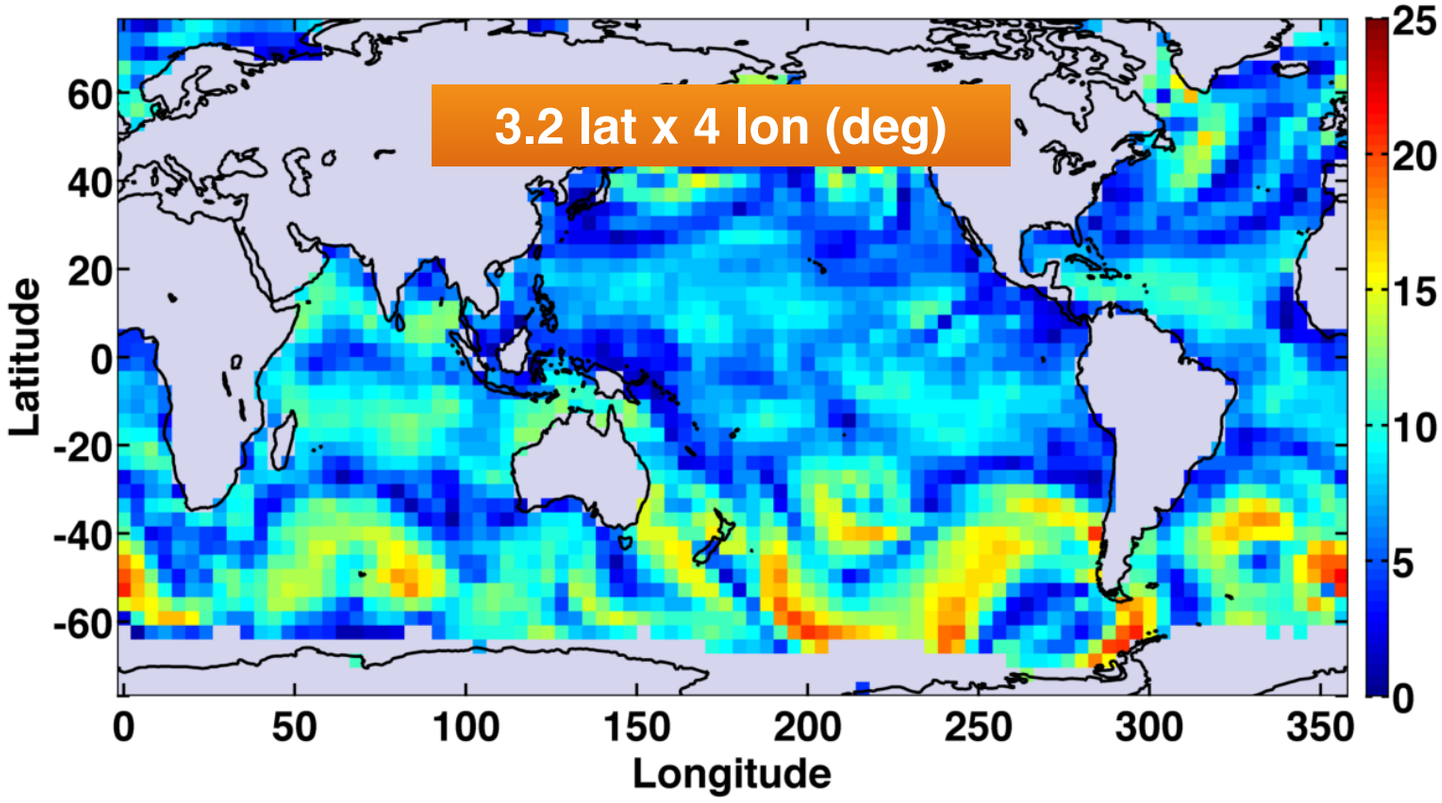

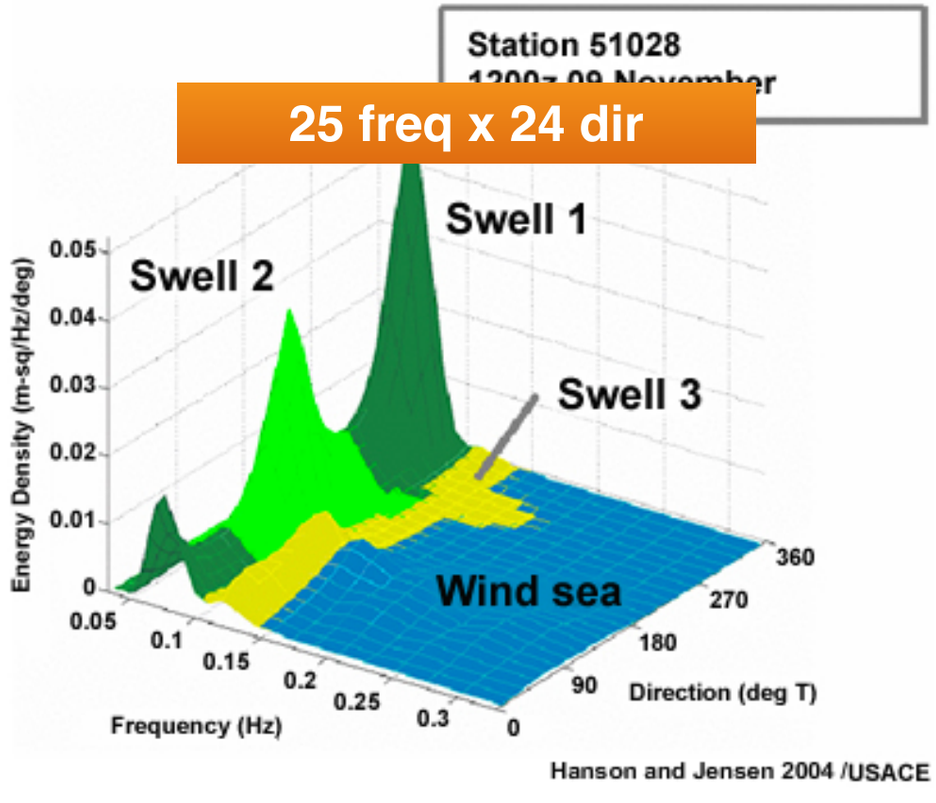

Figure: Sample spatial (SWH) and spectral output for the coupled NCAR CESM wave component.

Simple WAVEWATCH III cost analysis

WAVEWATCH III version 3.14

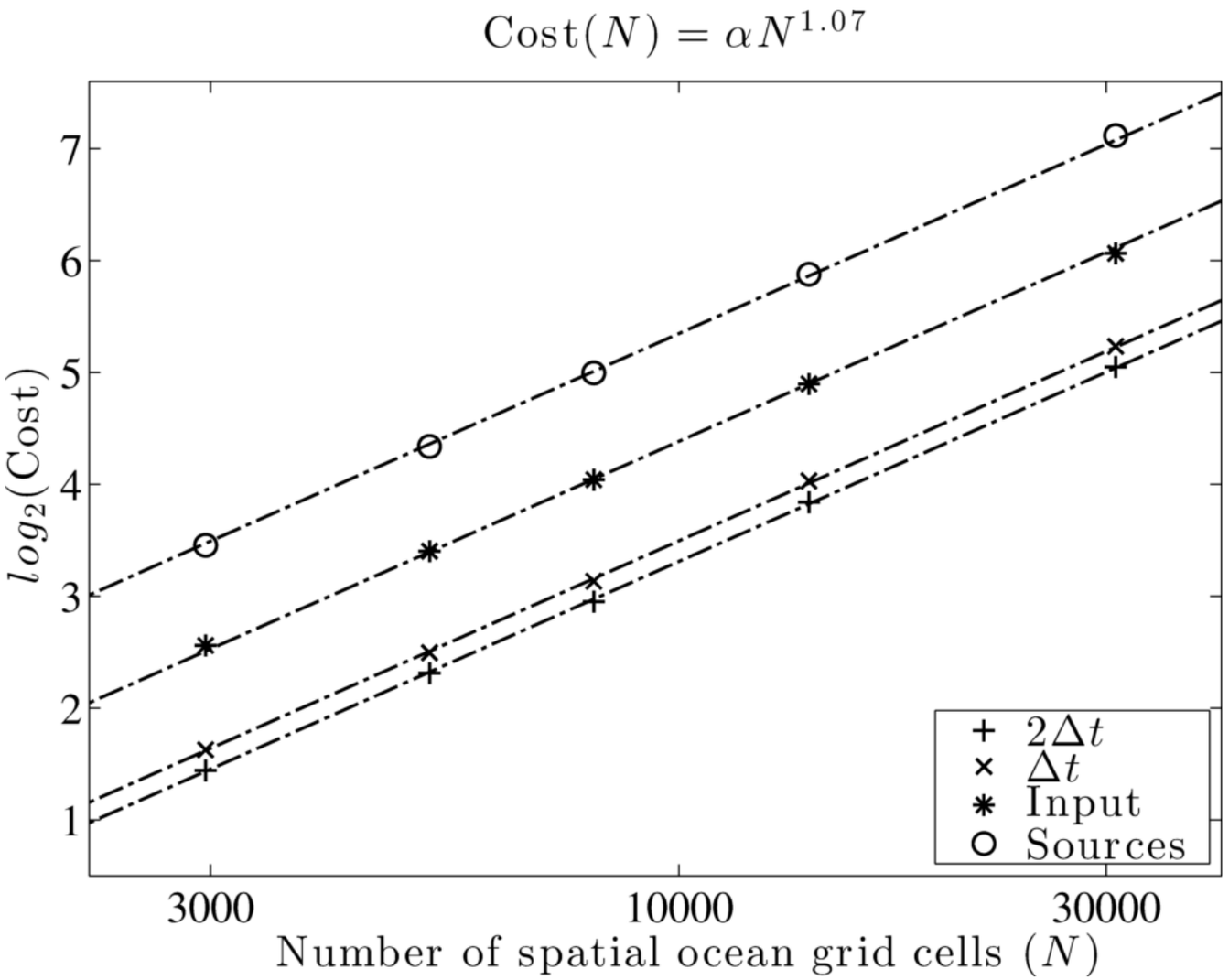

Figure: WAVEWATCH III cost versus spatial resolution using same time step and fixed spectral grid ($25f \times 24\theta$).

- Let N be the number of grid cells. Then running costs are

$$\mathrm{Cost}(N) = \alpha N^{1.07}.$$

- Using source terms approximately doubles cost since

$$\log_2[\mathrm{Cost}_{src}] \approx 1 + \log_2[\mathrm{Cost}_{in}]$$
$$\mathrm{Cost}_{src} \approx 2\,\mathrm{Cost}_{in}$$

- Changing grid resolution can have a dramatic effect on speed

$$N_{\mathrm{global}} = N_x \times N_y$$
$$N_{\mathrm{coarse}} = (N_x/3.2) \times (N_y/3.2)$$
$$\mathrm{Cost}_{\mathrm{global}} \approx 10\,\mathrm{Cost}_{\mathrm{coarse}}$$

Outline

1. Scientific background
2. Coupled wave component
3. Overview of meshless approach
4. Kinematic prototype
5. Discussion

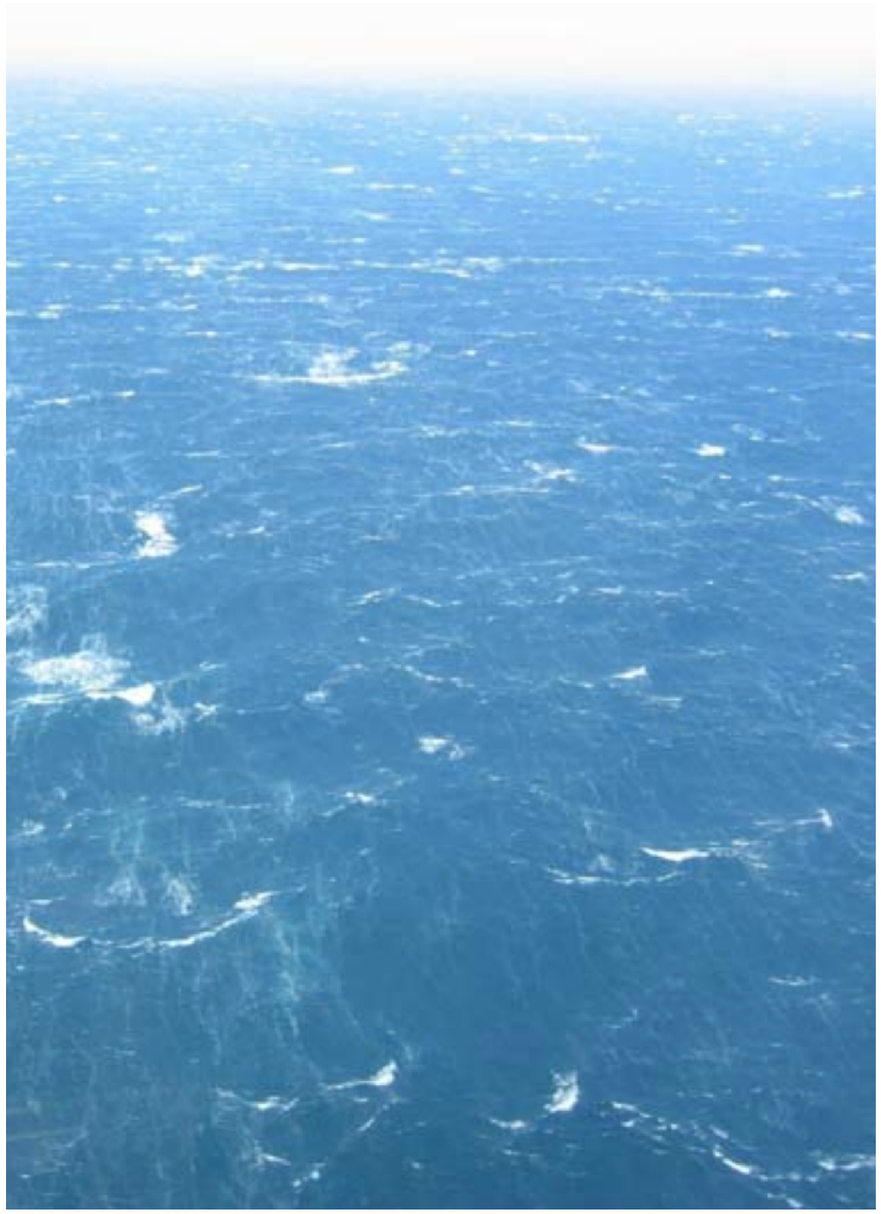

RBF and RBF-FD methods

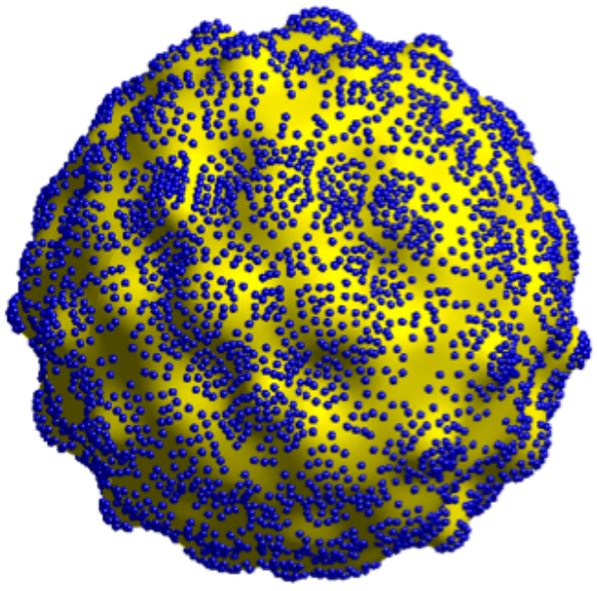

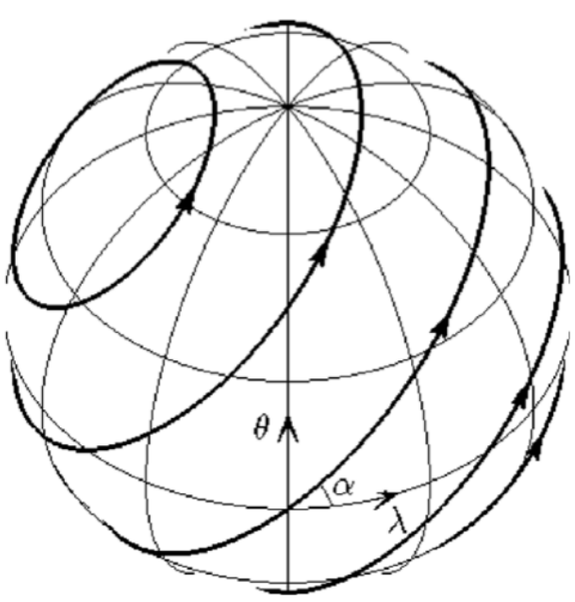

Figure: Example node layout of a bumpy sphere (Fuselier & Wright, 2012) and possible solid body rotation over the surface (Flyer & Wright, 2007)

Radial Basis Functions (RBF):

- Uses a meshless node layout
- Solves advective problems with spectral accuracy
- Allows geometric flexibility and local node refinement
- *No advective singularities*
- *Smooth solutions require much fewer unknowns compared with other methods*

RBF-Generated Finite Differences (RBF-FD):

- Uses local RBF-generated finite difference formulas to reduce memory count from $O(N^2)$ to $O(N)$
- Well-suited for parallelization (Bollig et al., 2012)

Solving PDEs with the local RBF-FD method

Local RBF-FD Method:

- Creates a set of FD weights (w) that are exact at point $\vec{\alpha}_s$ for the RBF (ϕ) centered at each node in the subset

$$\begin{bmatrix} \phi_{11} & \cdots & \phi_{1n} & 1 \\ \vdots & \ddots & \vdots & \vdots \\ \phi_{n1} & \cdots & \phi_{nn} & 1 \\ 1 & \cdots & 1 & 0 \end{bmatrix} \begin{bmatrix} w_1 \\ \vdots \\ w_n \\ w_{n+1} \end{bmatrix} = \begin{bmatrix} (\mathcal{L}\phi)_{s1} \\ \vdots \\ (\mathcal{L}\phi)_{sn} \\ 0 \end{bmatrix}$$

where $\phi_{ji} = \phi(\|\vec{\alpha} - \vec{\alpha}_i\|)|_{\vec{\alpha}=\vec{\alpha}_j}$

- Local weights are combined into a banded sparse matrix D such that

$$\begin{bmatrix} \mathcal{L}\mathcal{W}(\vec{\alpha}_1, t) \\ \vdots \\ \mathcal{L}\mathcal{W}(\vec{\alpha}_N, t) \end{bmatrix} \approx \begin{bmatrix} D_{11} & \cdots & D_{1N} \\ \vdots & \ddots & \vdots \\ D_{N1} & \cdots & D_{NN} \end{bmatrix} \begin{bmatrix} \mathcal{W}(\vec{\alpha}_1, t) \\ \vdots \\ \mathcal{W}(\vec{\alpha}_N, t) \end{bmatrix}$$

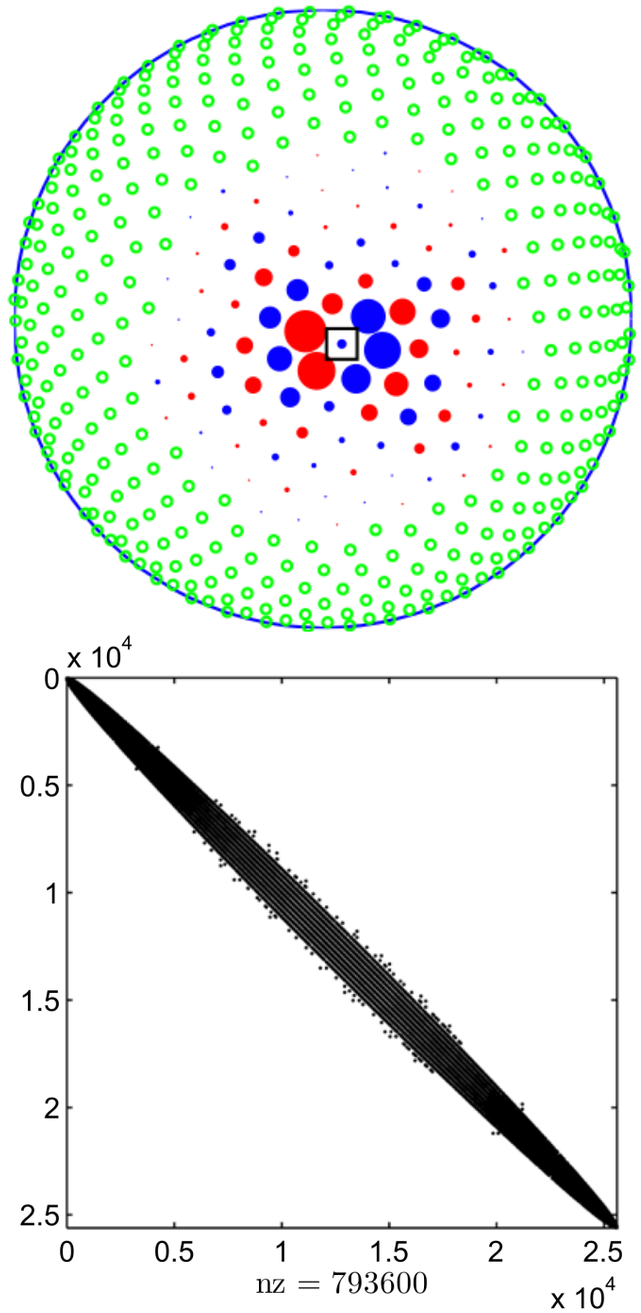

Figure: Sample (a) local differentiation weights and (b) global banded matrix (Flyer et al., 2012)

Stabilizing the RBF-FD method with hyperviscosity

Hyperviscosity Filter:

- A high-order Laplacian operator is used to stabilize the RBF-FD method

$$\partial_t \mathcal{W} = -D\mathcal{W} + \gamma \Delta^p \mathcal{W}$$

- The artificial diffusion coefficient is typically in the range of 10^{-20} to 10^{-45}

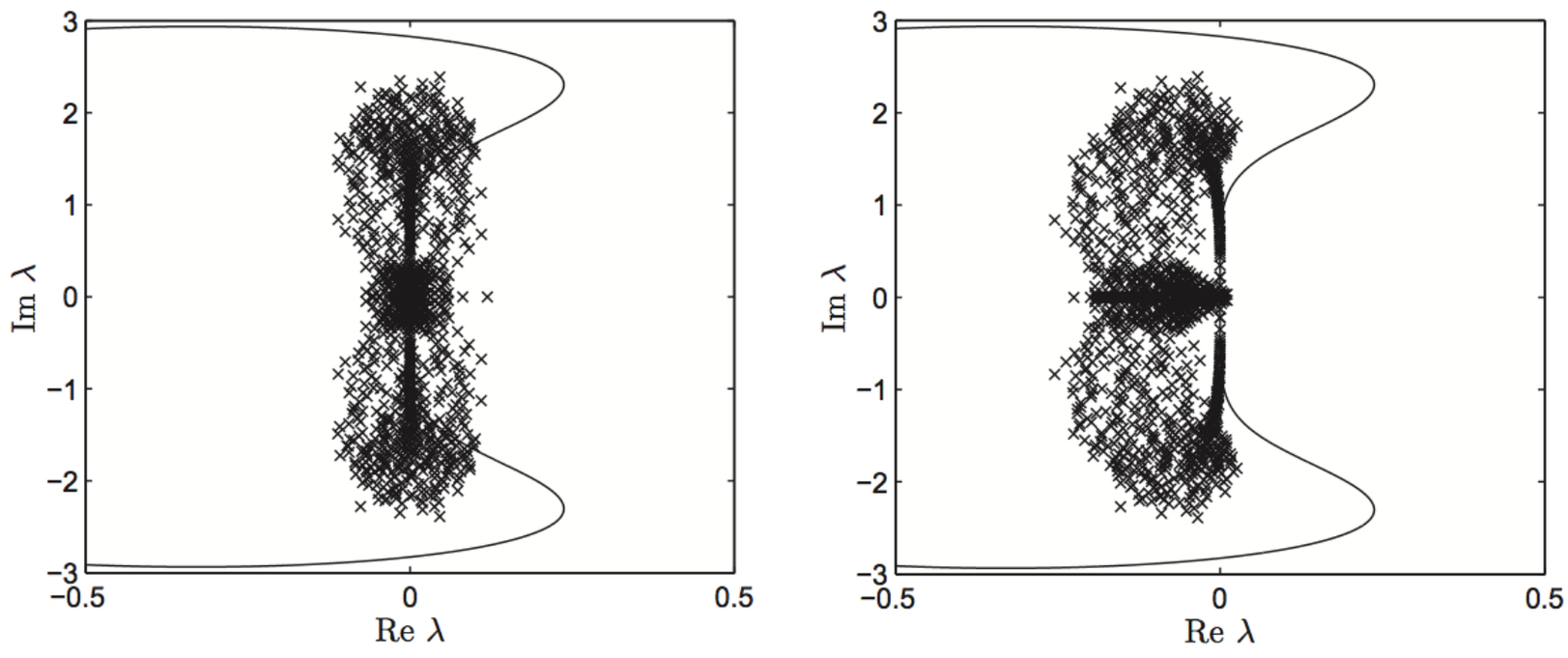

(a) No hyperviscosity (b) With hyperviscosity

Figure: Sample eigenvalue spectrum with the RK4 stability domain (solid line) (a) without hyperviscosity and (b) with a Δ^4-type hyperviscosity added. (Flyer et. al., 2012)

Outline

1. Scientific background
2. Coupled wave component
3. Overview of meshless approach
4. Kinematic prototype
5. Discussion

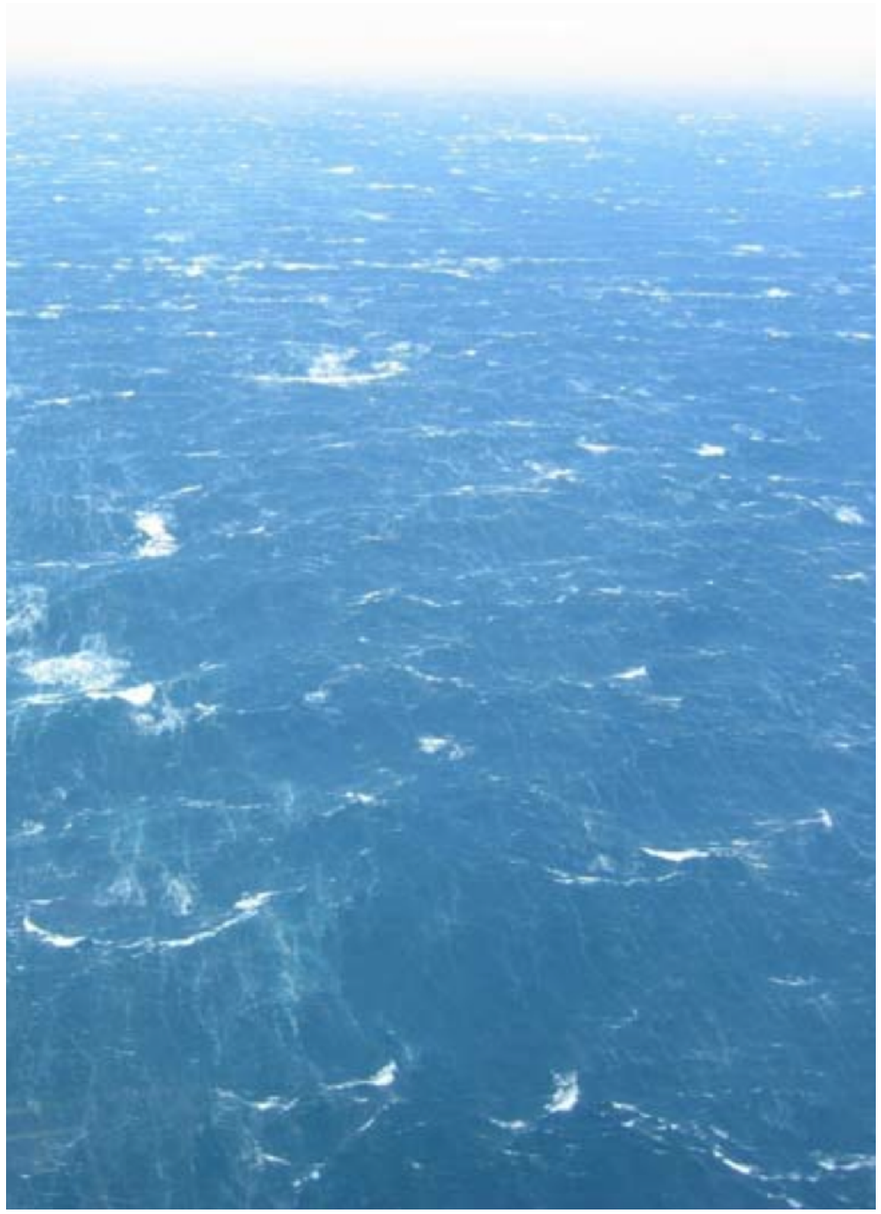

Coupled model domains

Spatial:

Directional-Frequency:

WAVEWATCH III:

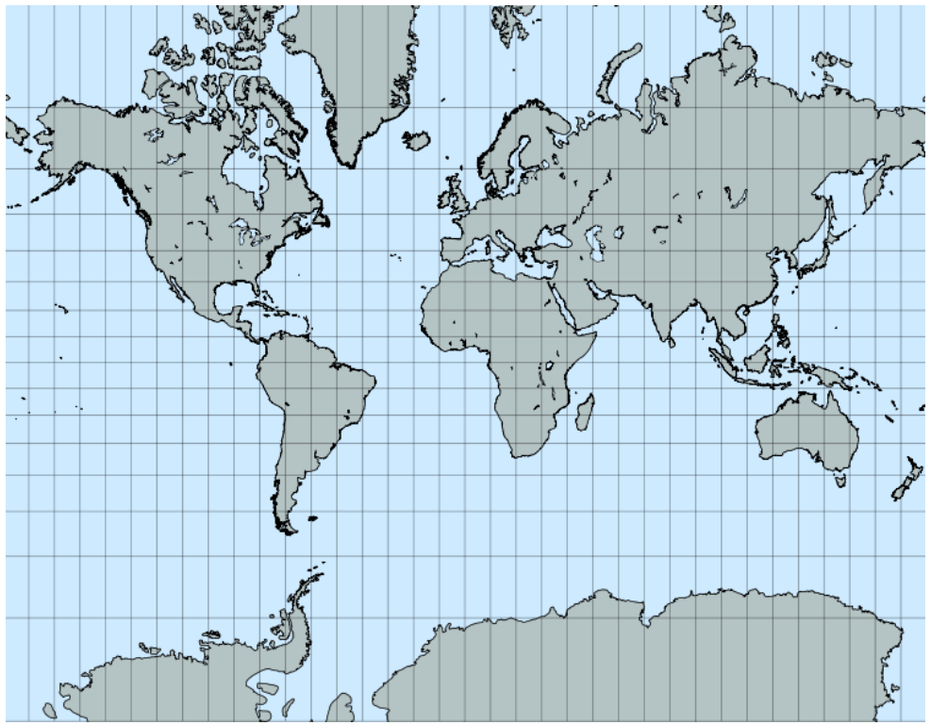

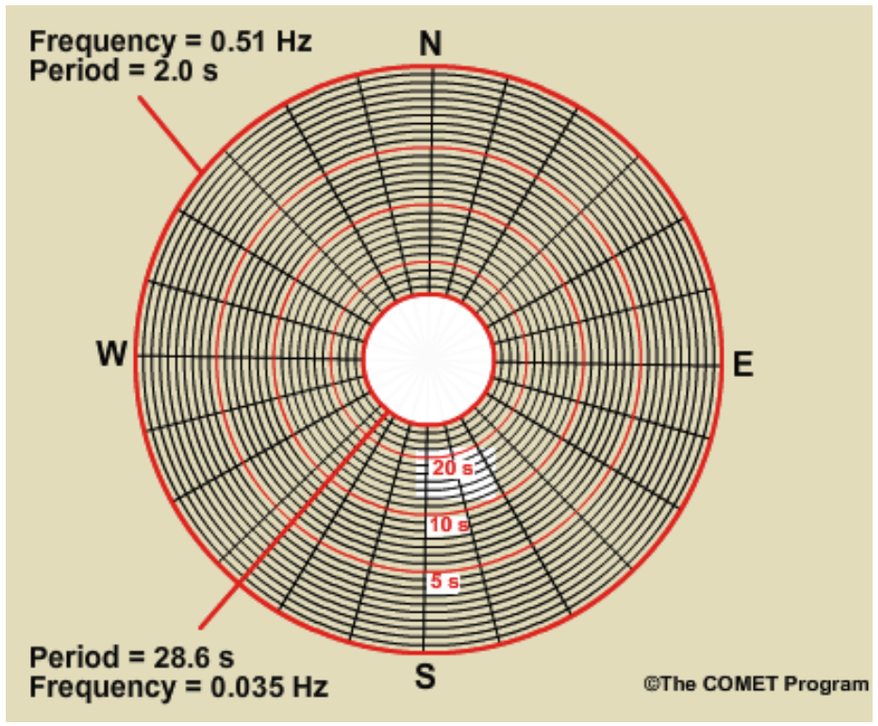

RBF-FD WAVE:

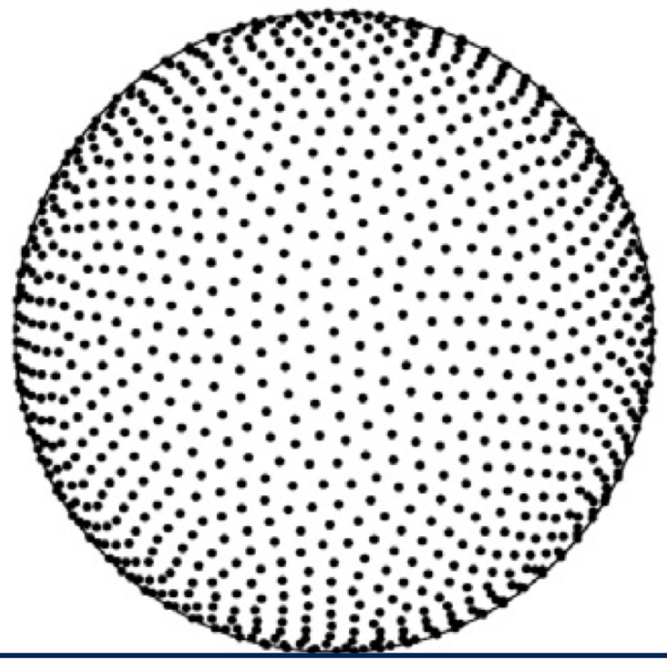

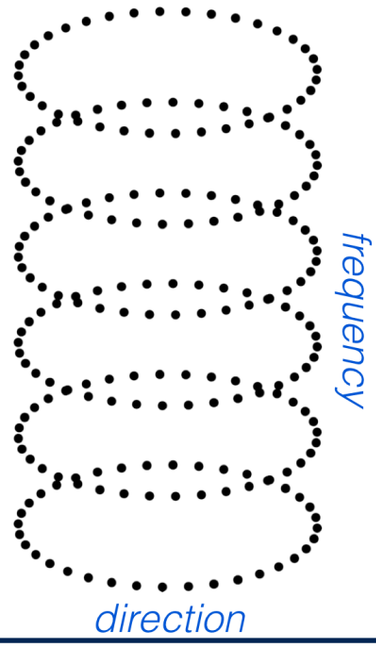

RBF-FD-W model (full-4D)

RBF-FD-W Details:

- $\phi(r) = e^{-(\varepsilon r)^2}$ for $\varepsilon, r \in \mathbb{R}_+^*$
- $\vec{\alpha} = (\vec{x}, \vec{k}) = (x, y, z, k_x, k_y, k_z)$

  $\Updownarrow$

  $\vec{\alpha} = (\vec{x}, \vec{f}) = (x, y, z, \theta_x, \theta_y, f)$
- Polar ice caps for latitudes above and below $\pm 75°$
- For constant depth with no currents, the wave action balance equation is given below:

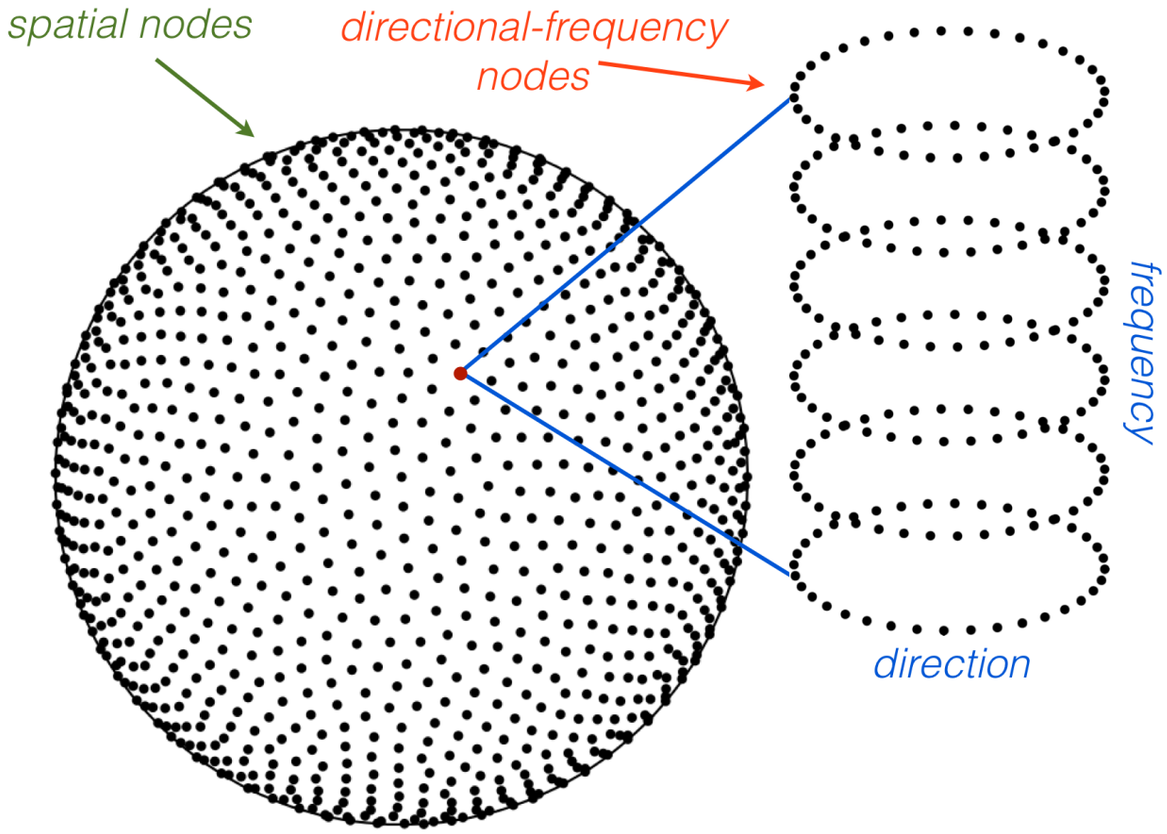

Figure: Sample coupled spatial and directional-frequency domain

$$\partial_t \mathcal{W} + \frac{\hat{c}_g(k_z)}{\sqrt{x^2+y^2}} \left\{ \left(-yk_x - xzk_y\right) \partial_x + \left(xk_x - yzk_y\right) \partial_y + k_y\left(x^2+y^2\right)\partial_z + \left(zk_x k_y\right) \partial_{k_x} + \left(-zk_x^2\right) \partial_{k_y} \right\} \mathcal{W}$$

$$= \text{Sources}$$

RBF-FD-W stencil selection (full-3D)

Convergence rates are determined by both the total number of nodes and local stencil size

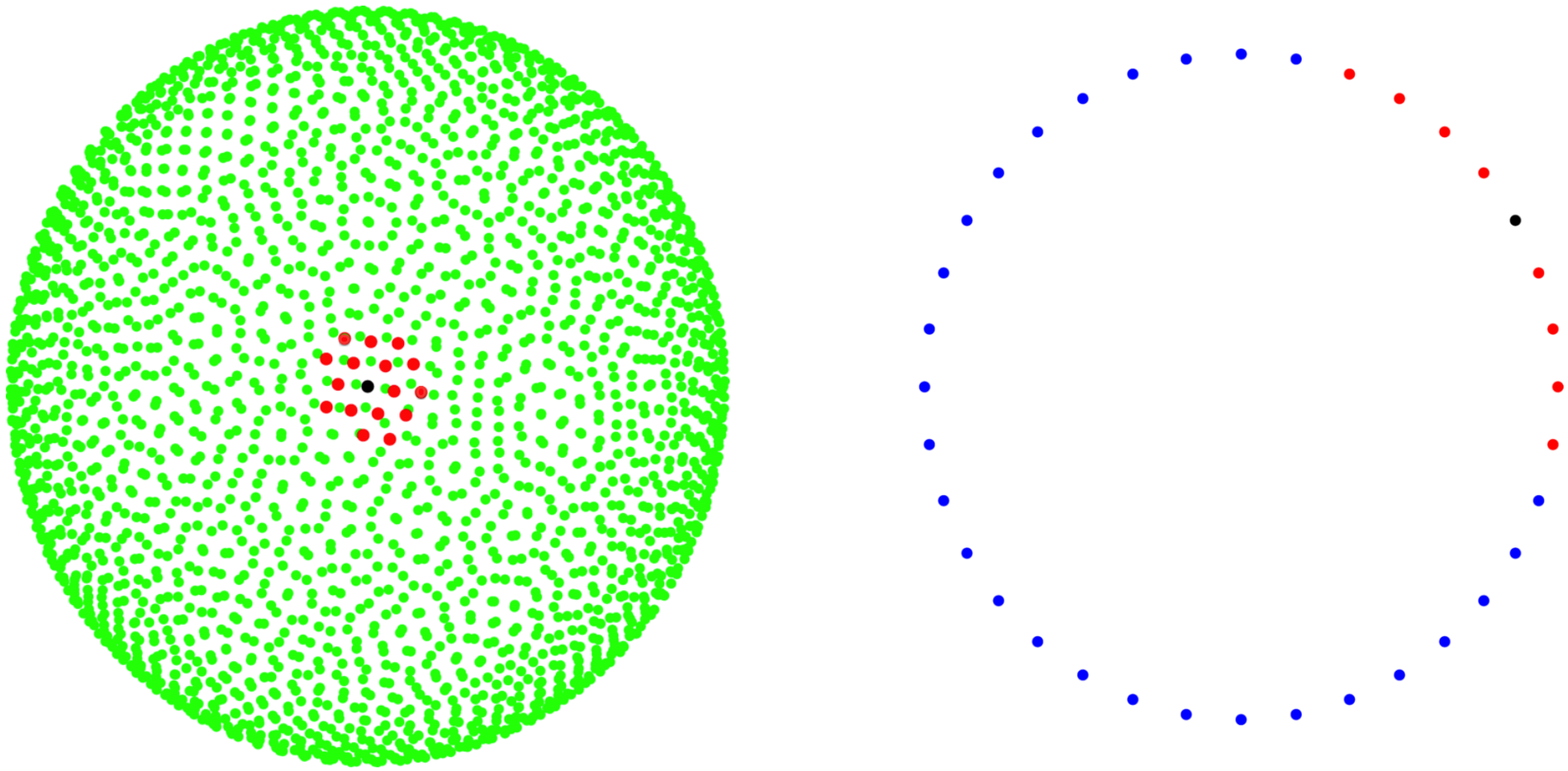

(a) Spatial stencil

(b) Directional stencil

Figure: Sample spatial and directional stencils for spatial node $(1, 0, 0)$ and dominant direction $\pi/6$. The combined stencil is $17_{\vec{x}} \times 9_{\vec{k}} = 153_{\vec{\alpha}}$.

Tuning: Spectral domain

Idealized spectra:

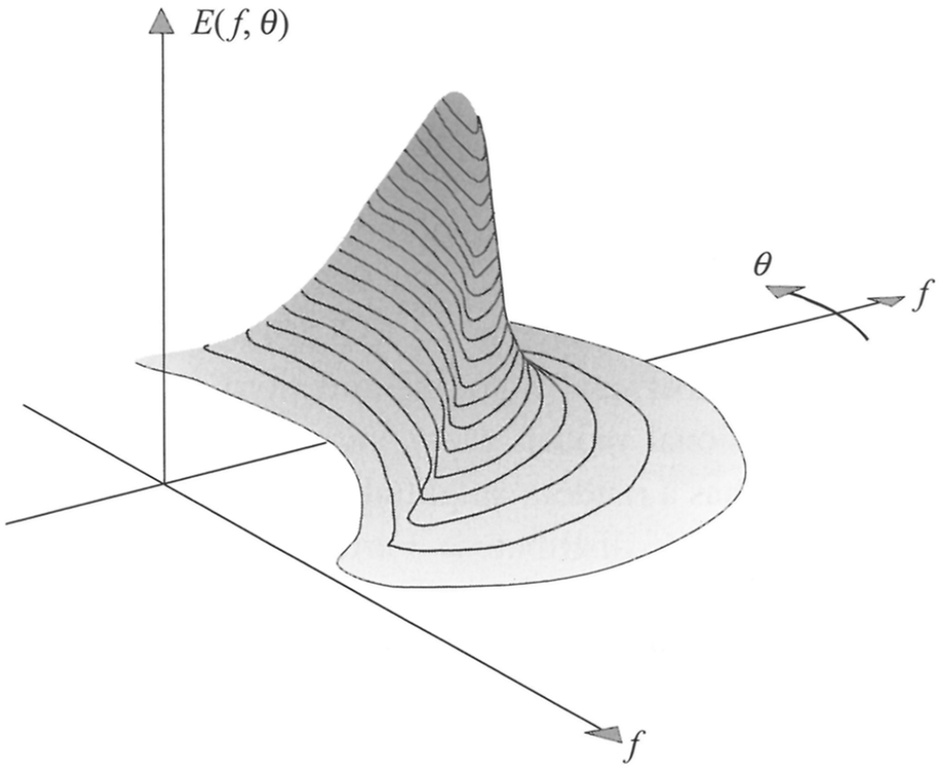

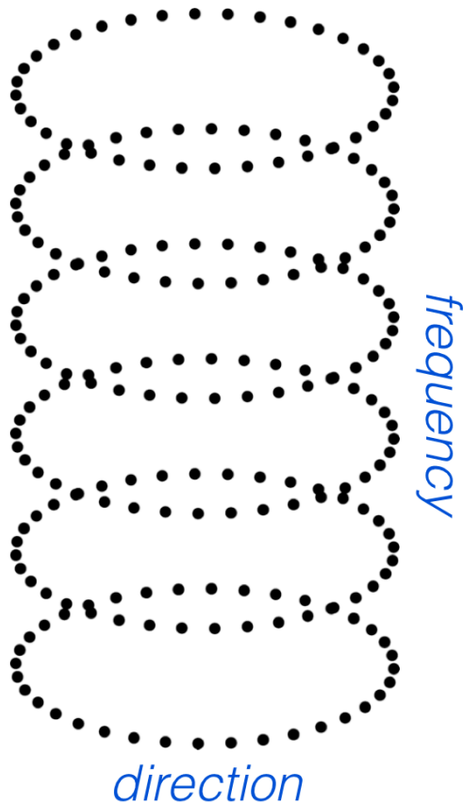

Spectral domain tuning details:

- Stencil sizes: 5, 7, 9, 11
- Global nodes: 24, 36, 48, 60
- Initial bell widths: 60 - 180 deg

Initial conditions:

Type	Equation	Normalization
Gaussian bell	$\mathcal{W}_0(\theta) = \exp[-(9\theta/2d)^2]$	$(2\sqrt{\pi}d/9)\,\mathrm{erf}[9\pi/2d]$
Cosine bell	$\mathcal{W}_0(\theta) = \cos^2[\pi\theta/d]$	$d/2$
	for $\lvert\theta\rvert < d/2$; 0 otherwise	

Tuning: Spectral domain

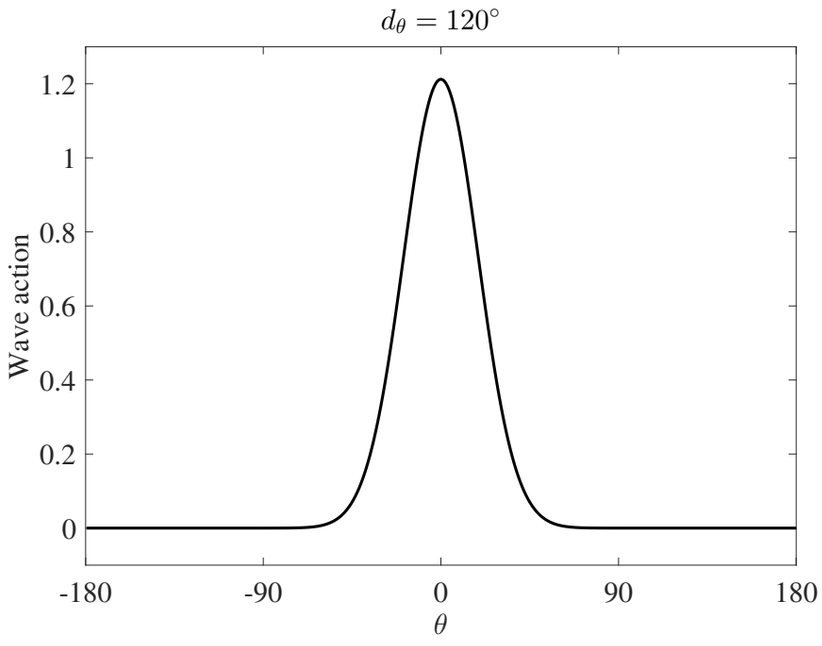

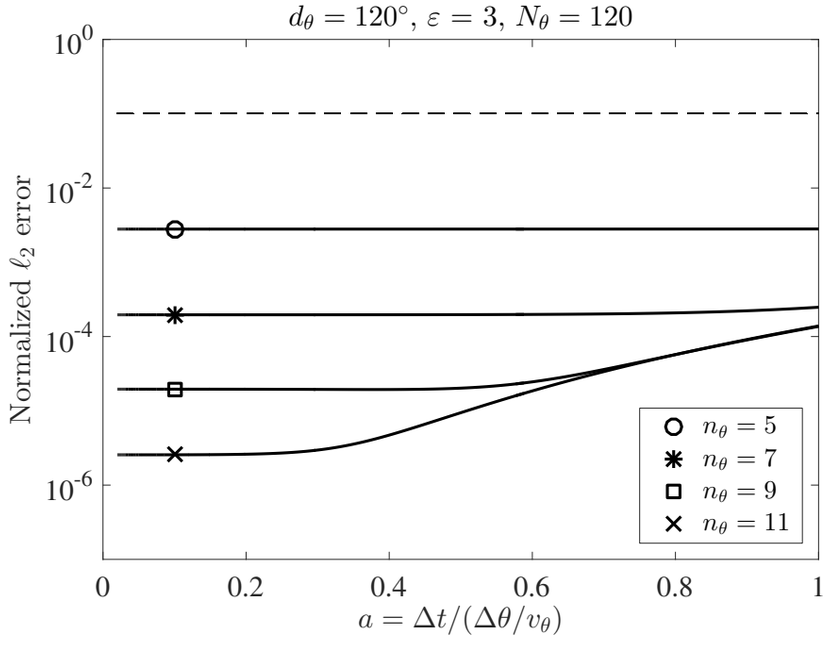

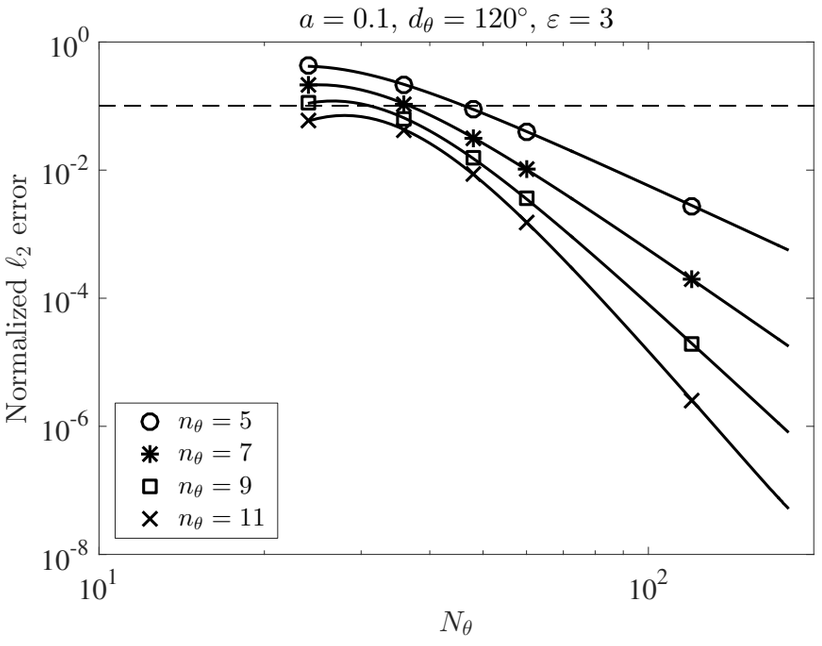

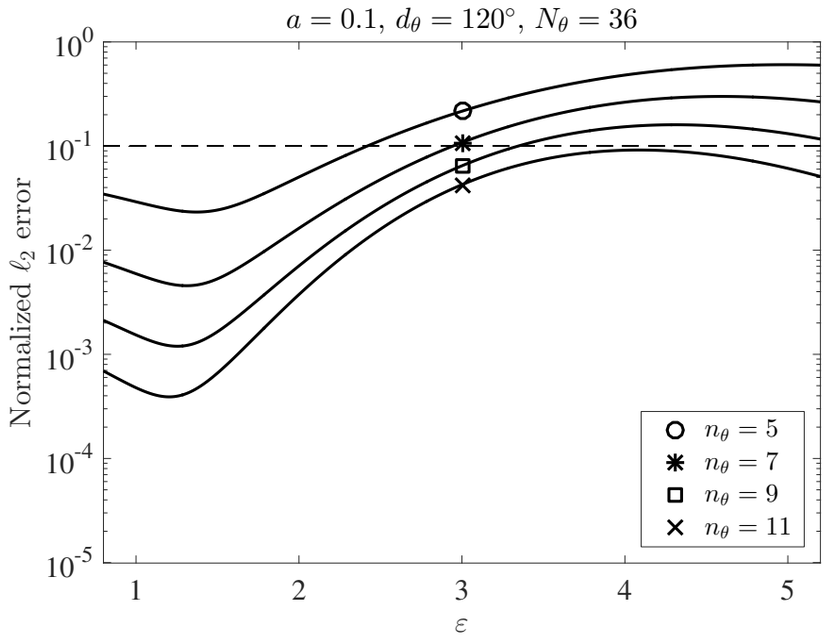

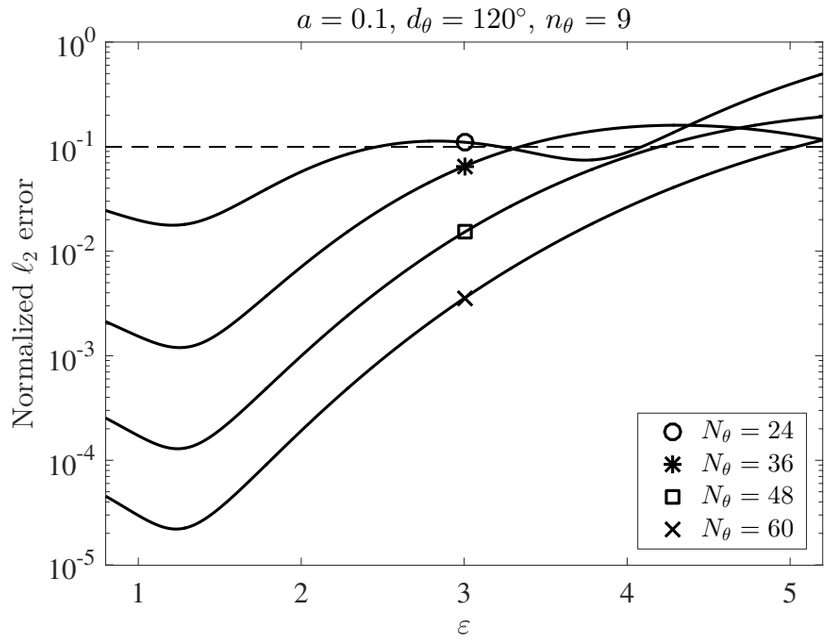

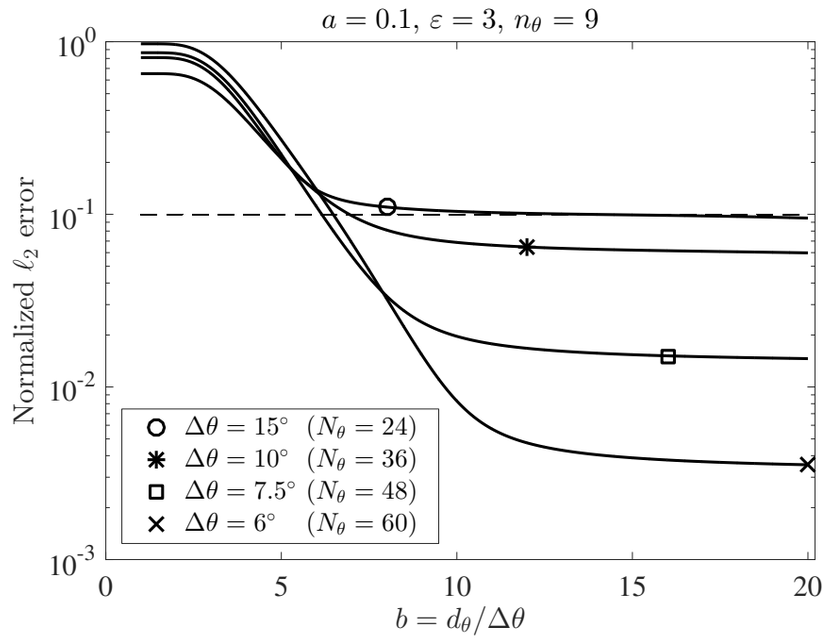

Figure: Spectral advection test with (a) Gaussian bell initial condition and (b-f) relative ℓ_2 errors after 1/4 revolution.

Tuning: Spatial domain

Width = 60 deg

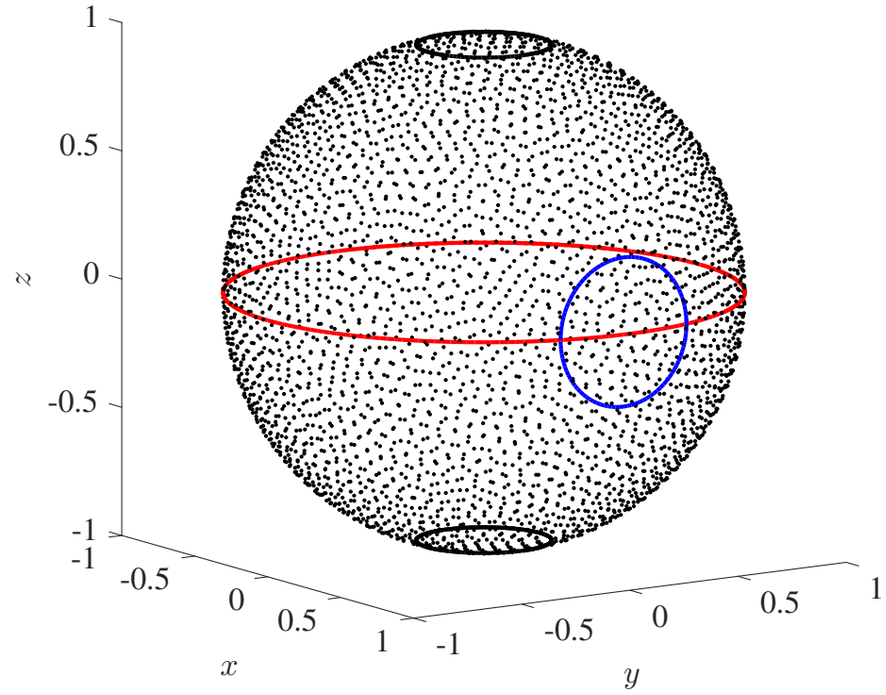

Width = 30 deg

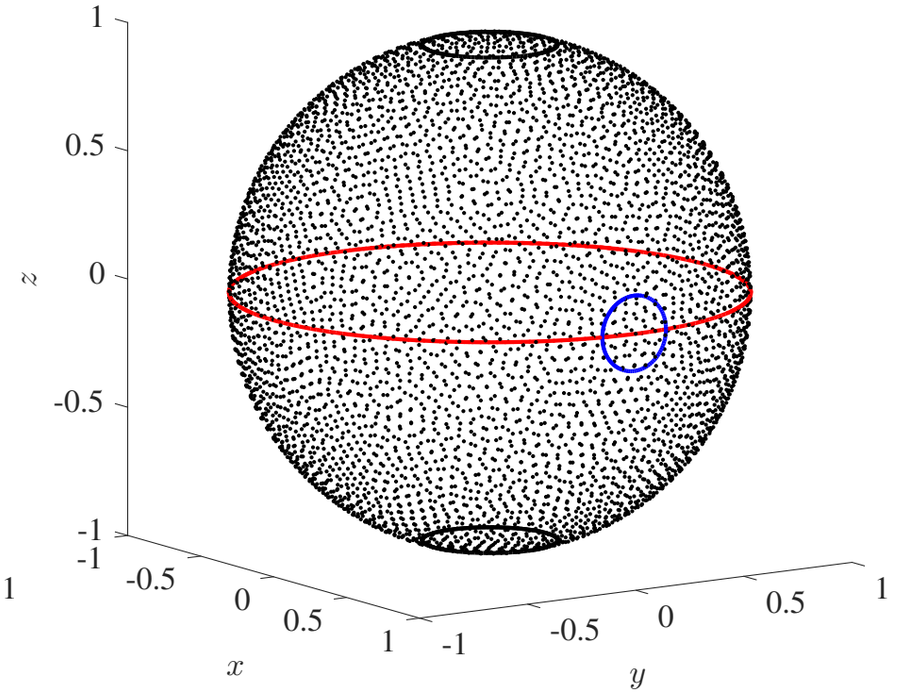

Spatial domain tuning details:

- Stencil sizes: 17, 31, 50
- Global nodes: 2500, 3600, 4900
- Initial bell widths: 45 - 60 deg

Initial conditions:

Type	Equation	Normalization
Gaussian bell	$\mathcal{W}_0(\theta) = \exp[-(9\theta/2d)^2]$	$(2\sqrt{\pi}d/9)\,\mathrm{erf}[9\pi/2d]$
Cosine bell	$\mathcal{W}_0(\theta) = \cos^2[\pi\theta/d]$	$d/2$
	for $\lvert\theta\rvert < d/2$; 0 otherwise	

Tuning: Spatial domain

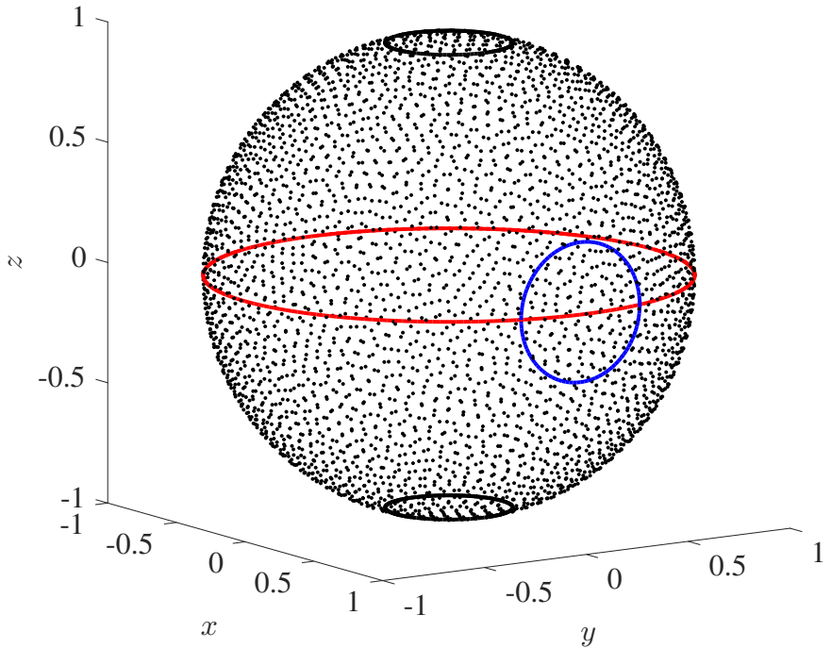

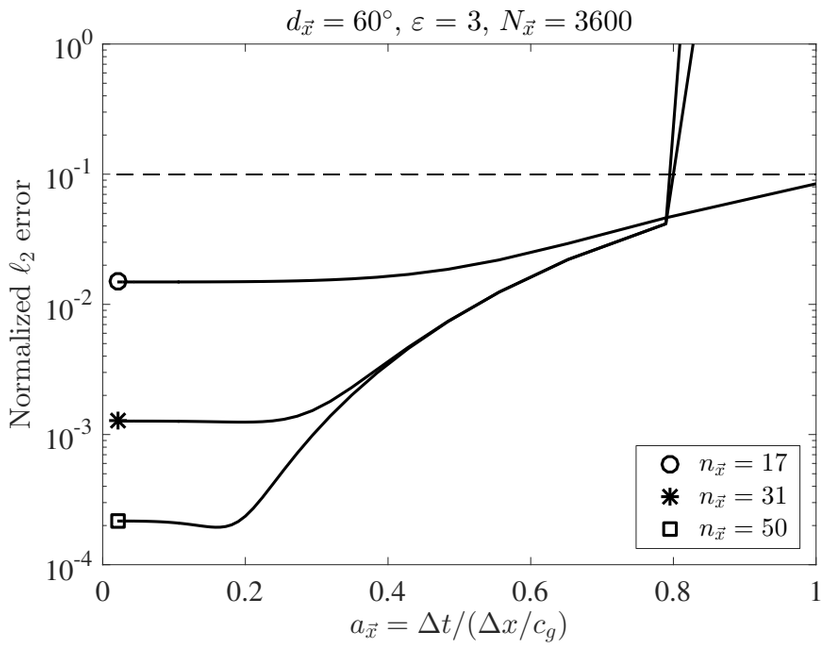

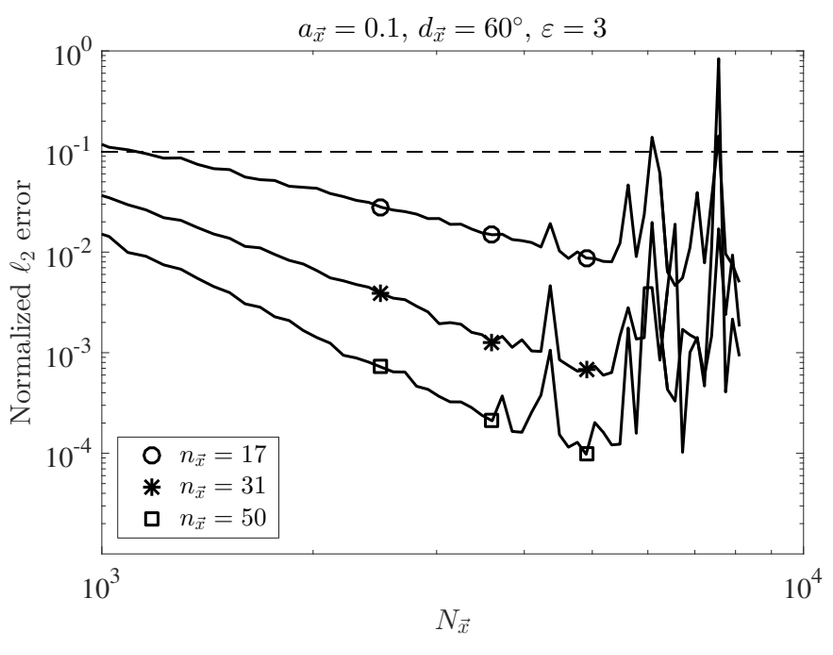

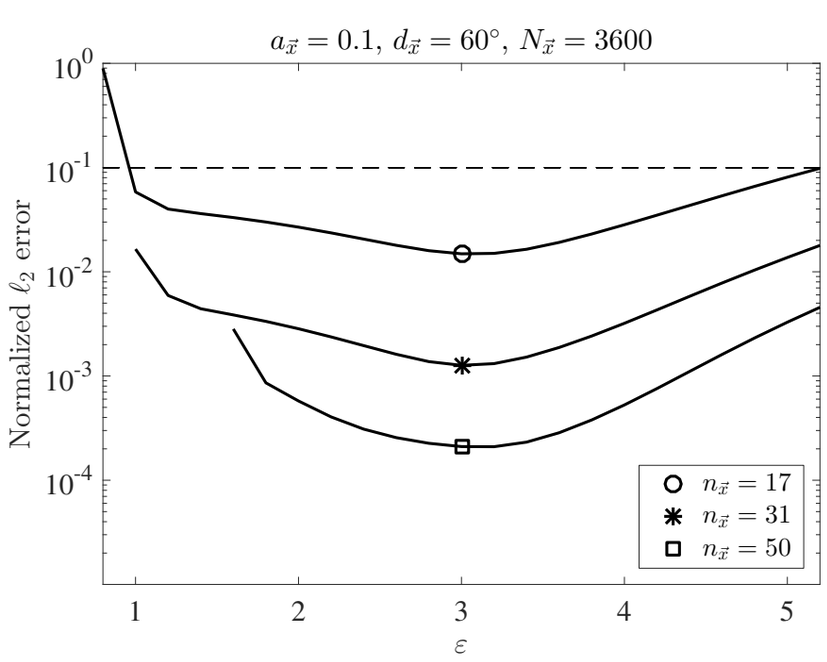

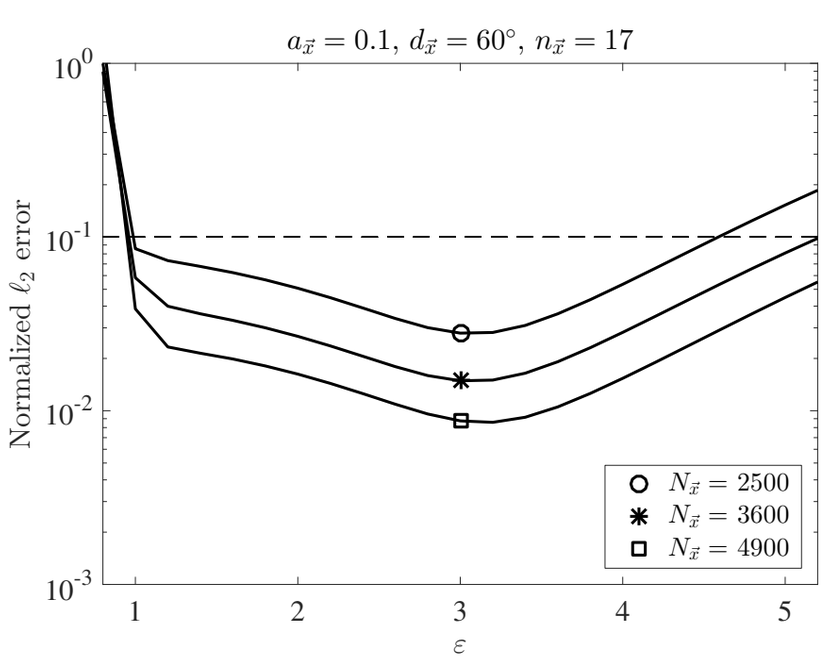

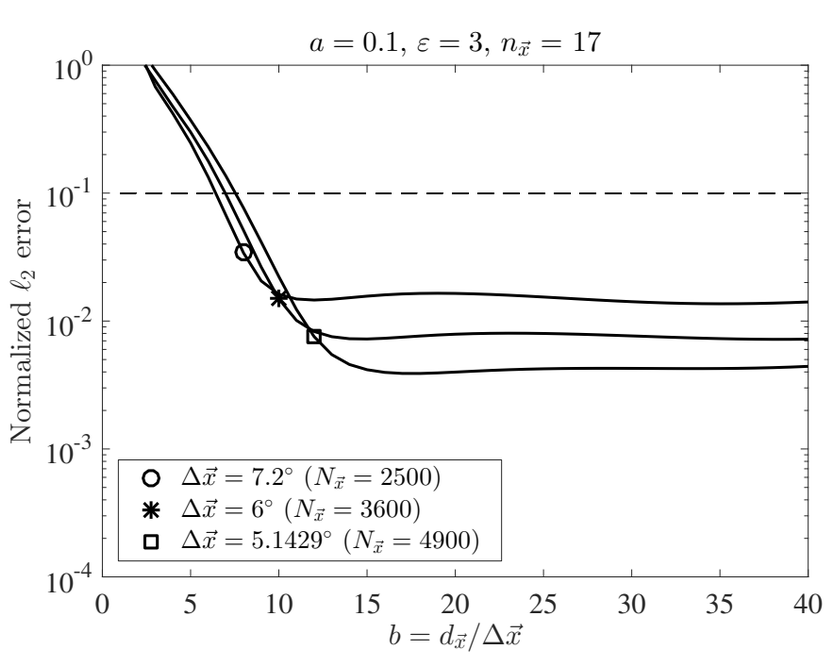

Figure: Spatial advection test along equator with (a) Gaussian bell initial condition and (b-f) relative ℓ_2 errors after 1/2 revolution.

Advection in the coupled domains

Test initialized with a spatial and directional Gaussian bell and a 30° dominant direction

$3600_{\vec{x}} \times 36_{\vec{k}}$ global nodes with $17_{\vec{x}} \times 9_{\vec{k}}$ stencil

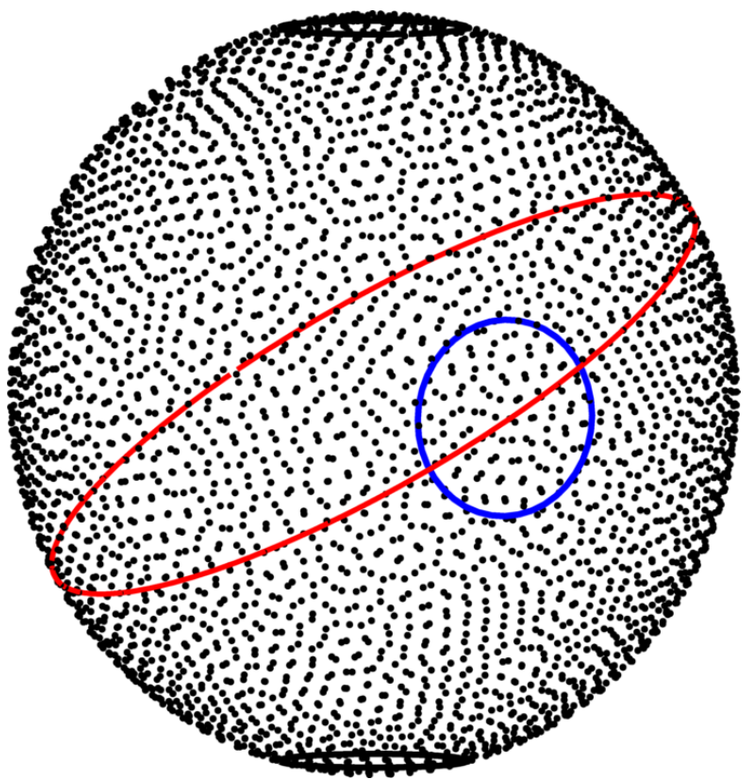

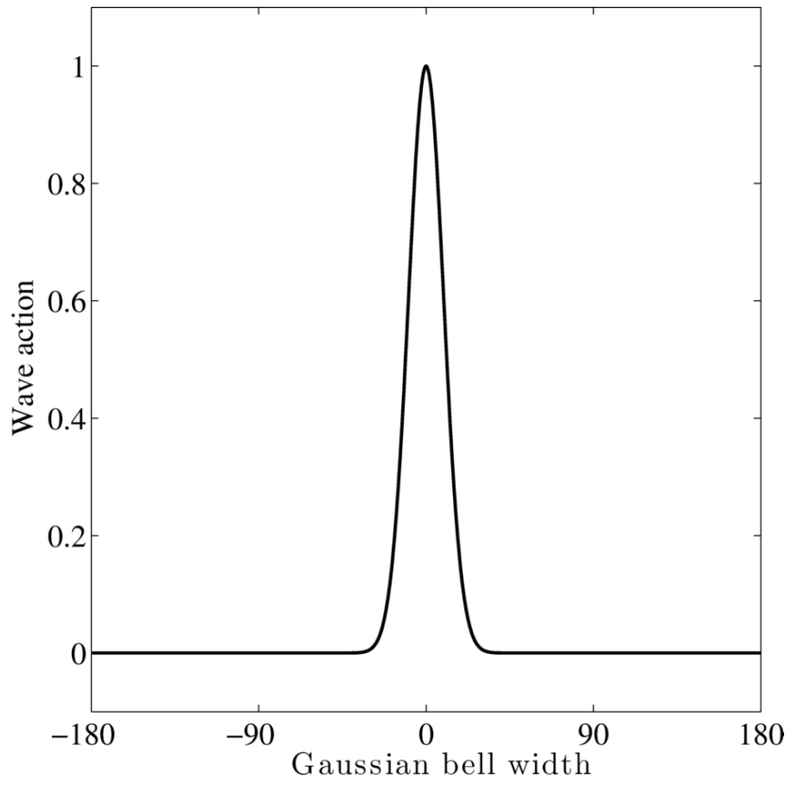

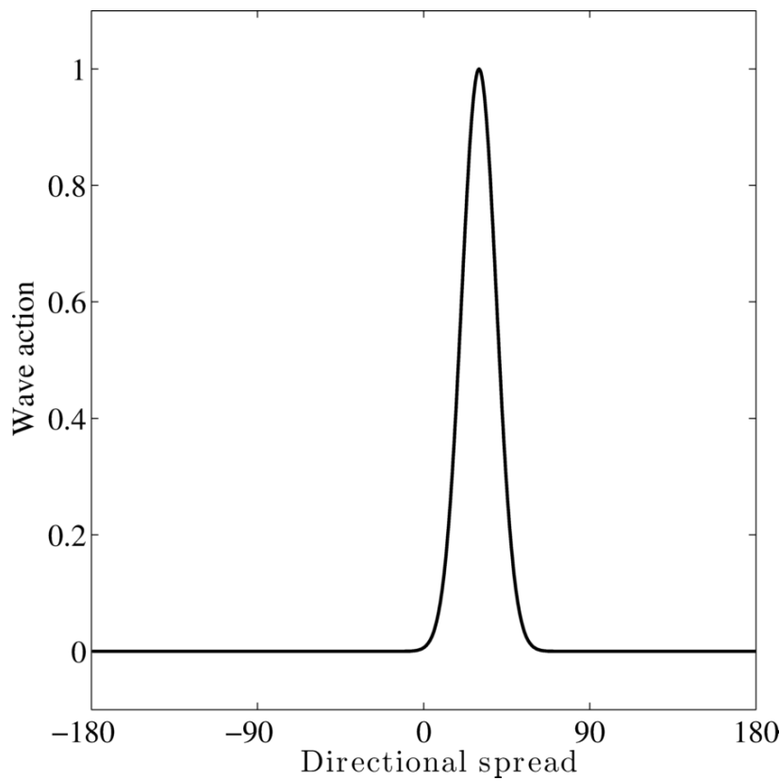

Figure: (a) Node set with advection path (red), peak Gaussian bell edge (blue), and ice edges (black); (b) initial spatial Gaussian profile; (c) directional spread about dominant direction

Spectral advection in coupled domain

$3600_{\vec{x}} \times 36_{\vec{k}}$ global nodes with $17_{\vec{x}} \times 9_{\vec{k}}$ stencil

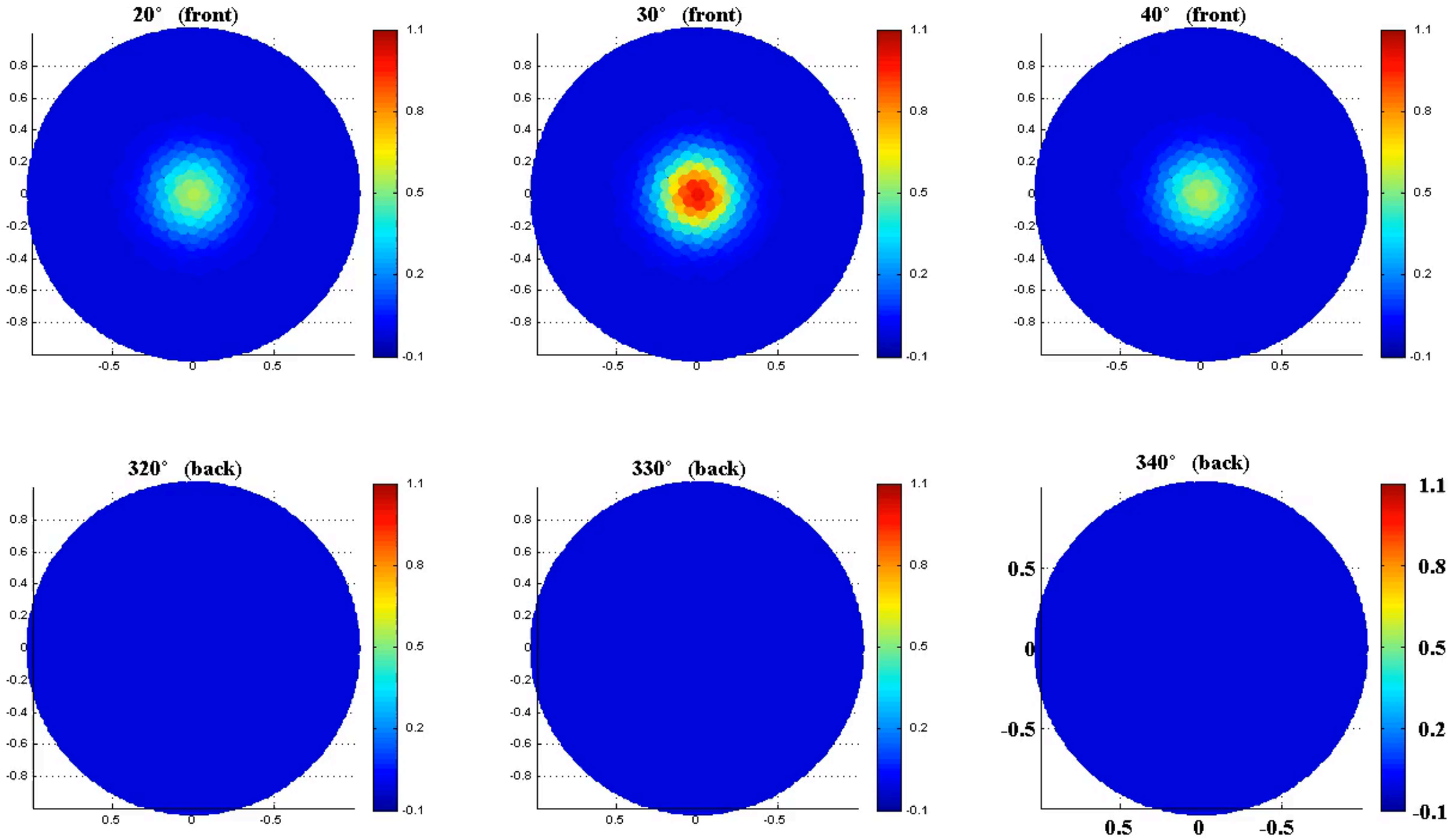

Figure: Select directional node values initialized with a spatial and directional Gaussian bell (60° width).

Initial direction error comparison

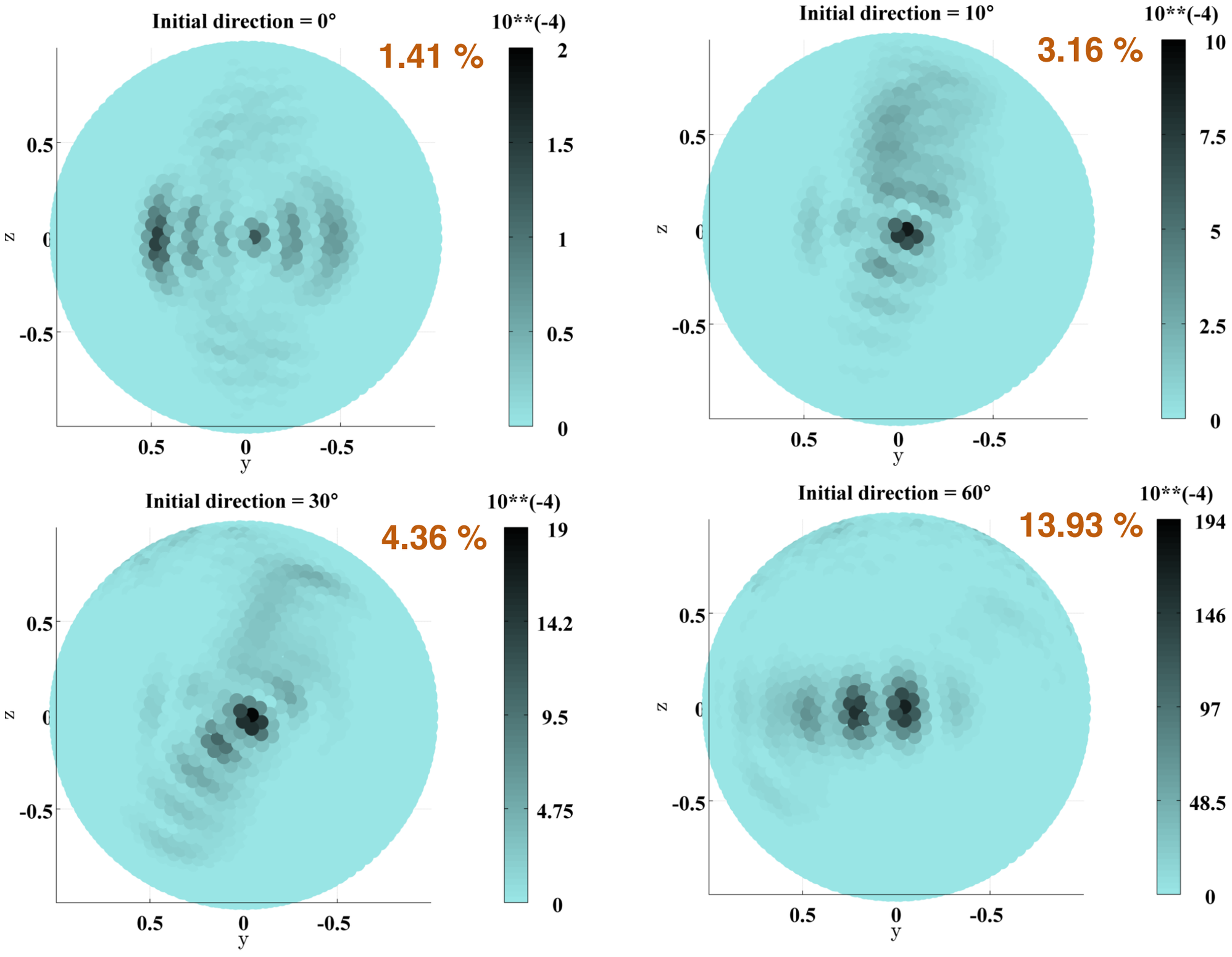

Figure: Relative ℓ_2^2 errors after 1/2 revolution for select **initial directions**.

Global node error comparison

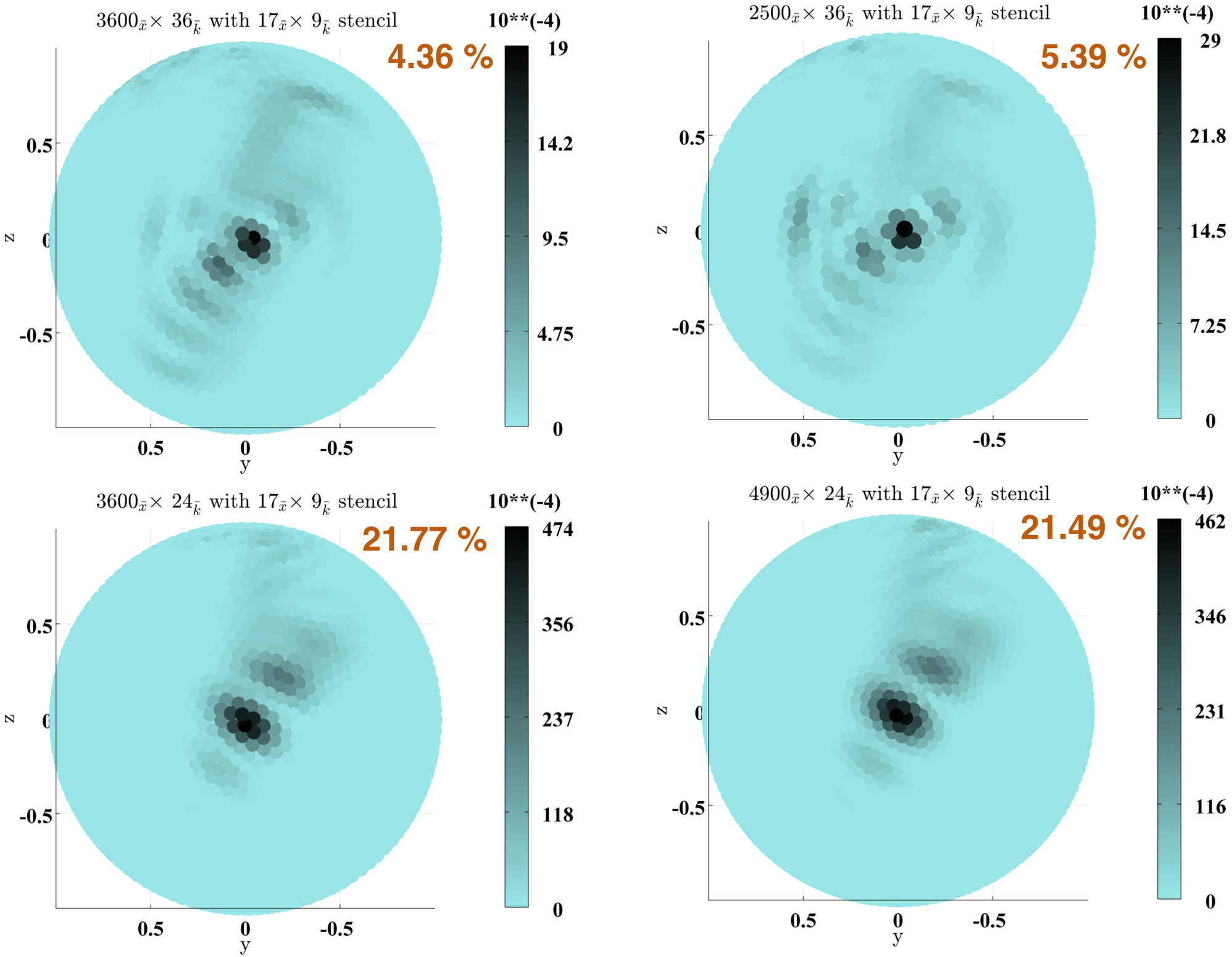

Figure: Relative ℓ_2^2 errors after 1/2 revolution for select **global node sets**.

Moment advection in the coupled domain

$3600_{\vec{x}} \times 36_{\vec{k}}$ global nodes with $17_{\vec{x}} \times 9_{\vec{k}}$ stencil

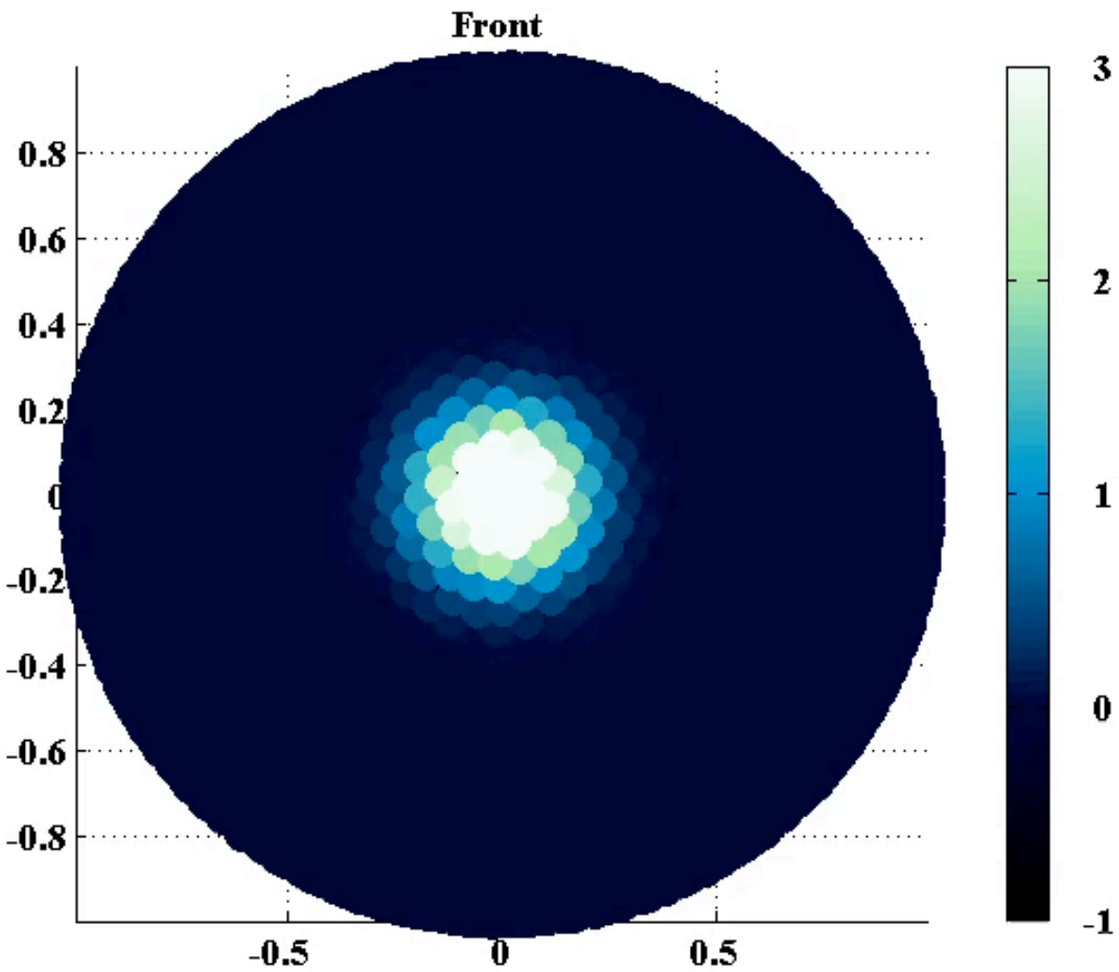

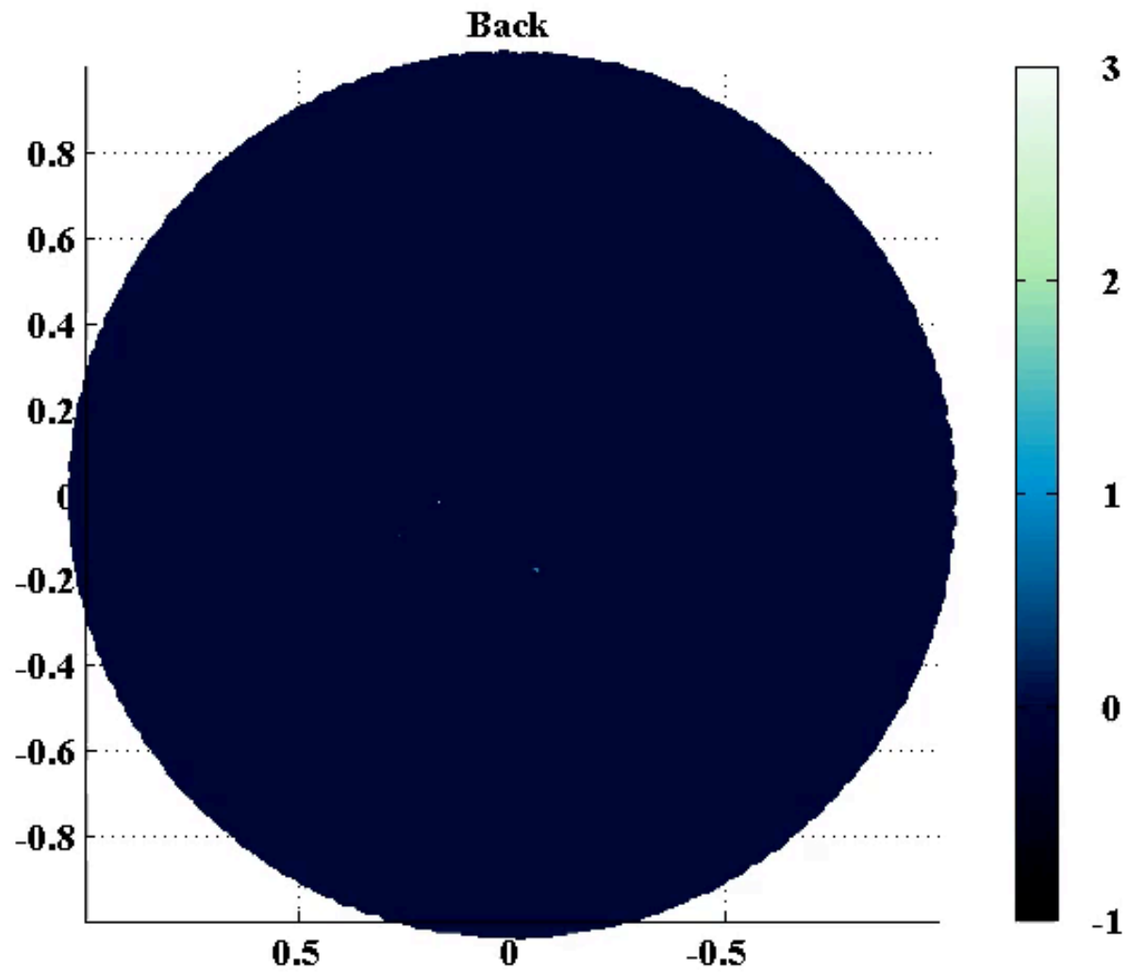

Figure: Integrated wave action ($Hm_0^2/16$) initialized with a spatial and directional Gaussian bell (45° and 120° width) and 20° dominant direction

Coupled model domains

Spatial:

Directional-Frequency:

WAVE- WATCH III:

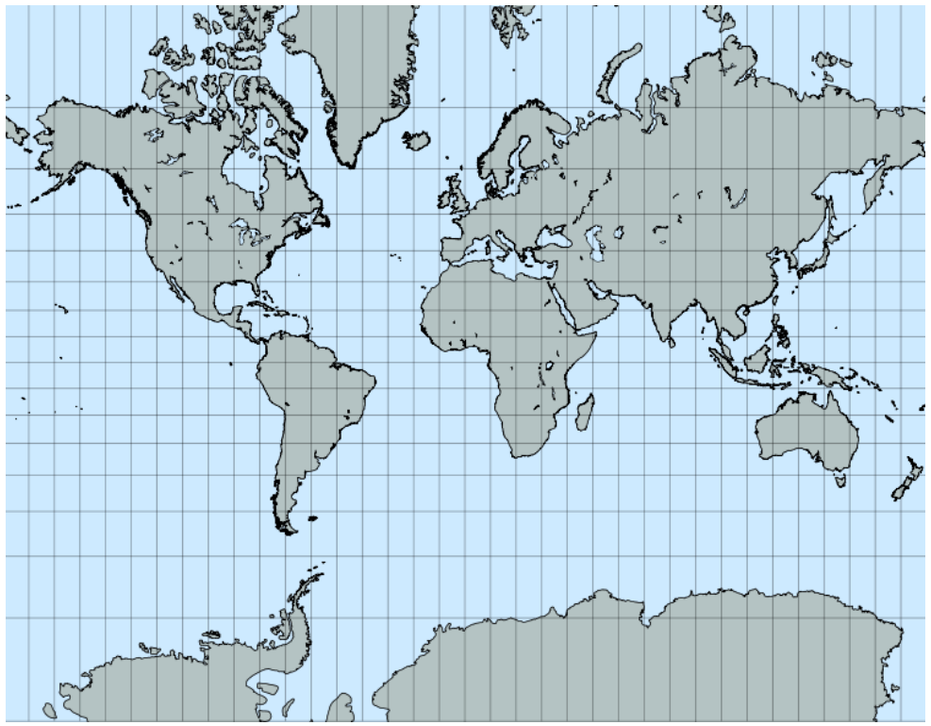

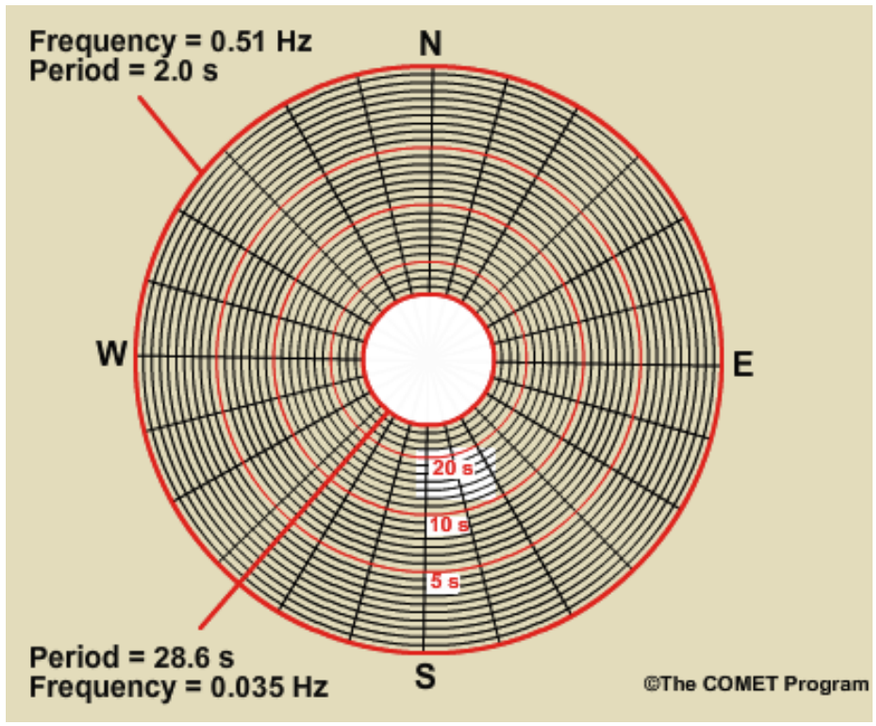

RBF-FD WAVE:

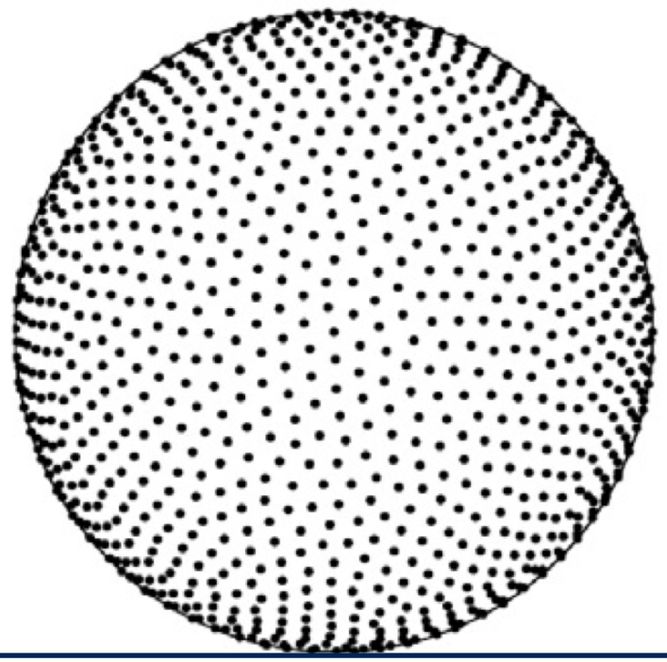

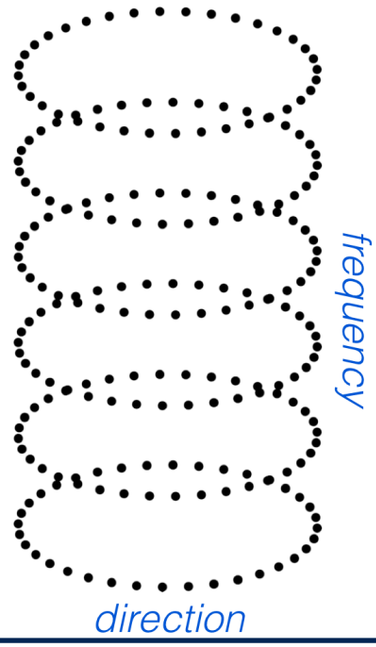

WAVEWATCH III comparison

$N_{\vec{x}} = 4320$, revolution $= 1/2$, dominant direction $= -30°$

Solution

$4° \times 3.25°$ $(N_{\bar{x}} = 4320)$

WW3

$4° \times 3.25°$ $(N_{\bar{x}} = 4320)$

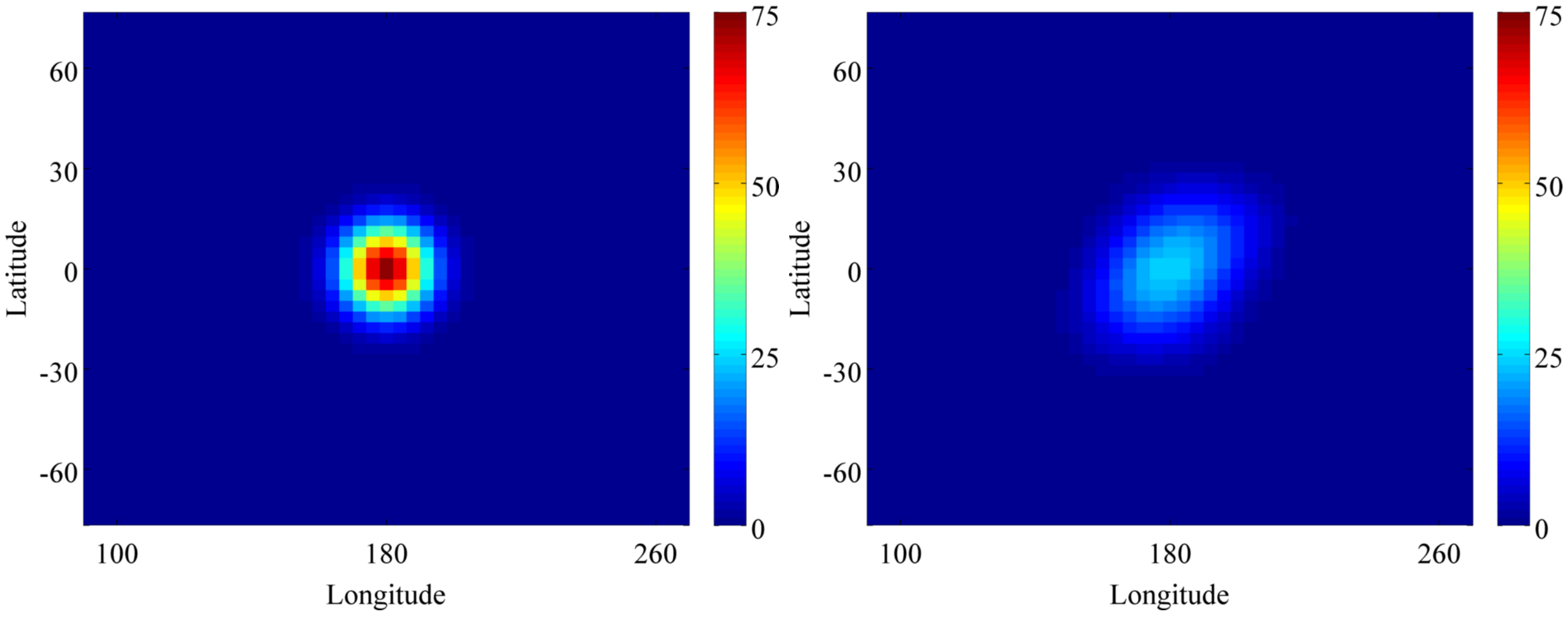

Figure: Selected directional grid cell value initialized with a spatial Gaussian (57.2° width) and directional cosine-20-power (64° width) after 1/2 revolution. The significant wave height is 2.5 m.

WAVEWATCH III comparison

$N_{\vec{x}} = 44064$, revolution $= 1/2$, dominant direction $= -30°$

Solution

$1.25° \times 1°$ $(N_{\bar{x}} = 44064)$

WW3

$1.25° \times 1°$ $(N_{\bar{x}} = 44064)$

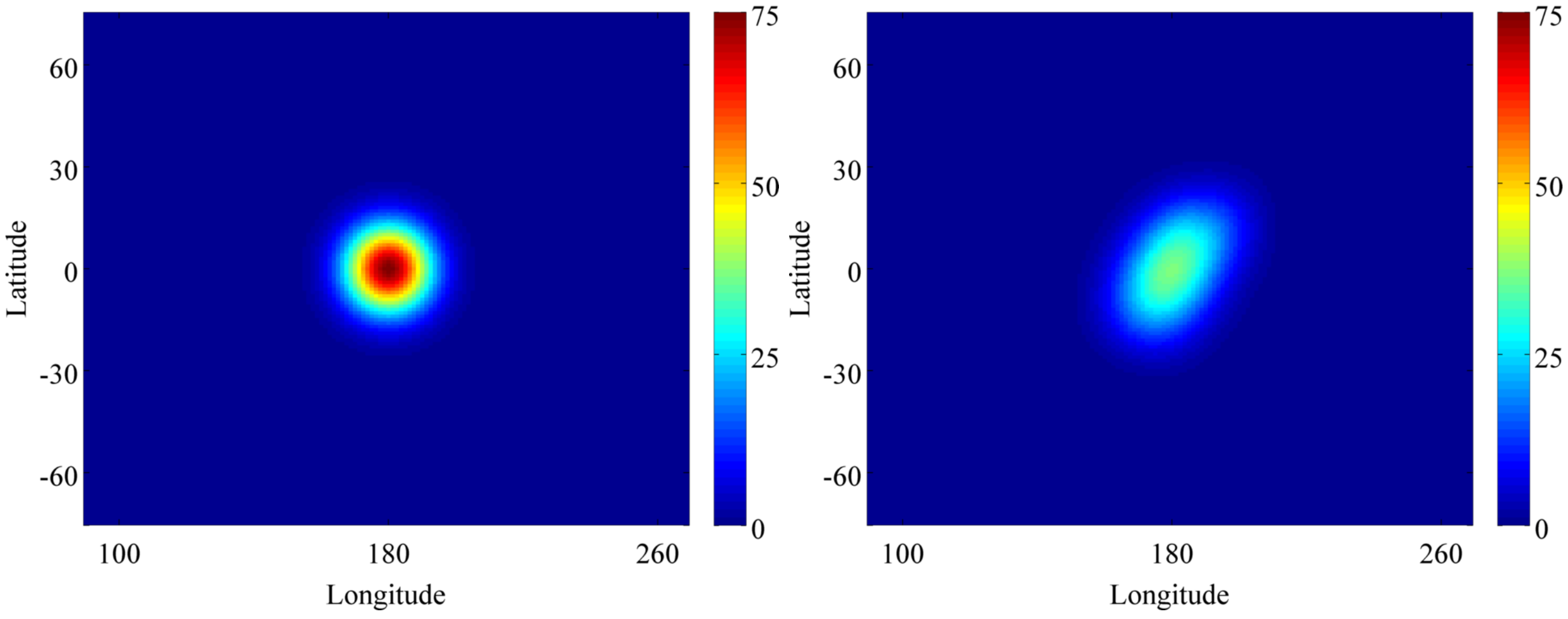

Figure: Selected directional grid cell value initialized with a spatial Gaussian (57.2° width) and directional cosine-20-power (64° width) after 1/2 revolution. The significant wave height is 2.5 m.

WAVEWATCH III error

Relative total ℓ_2^2 errors over all directions

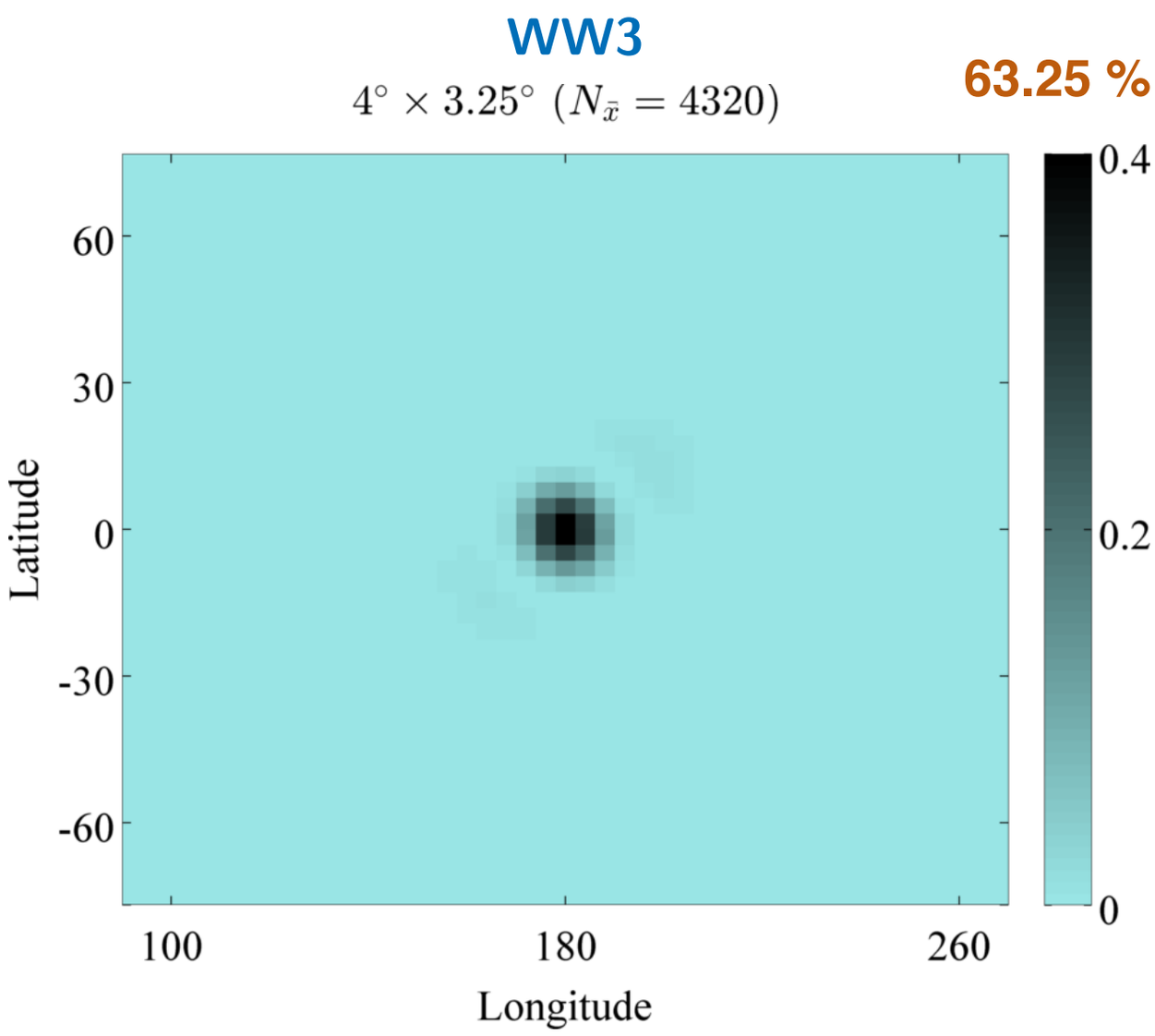

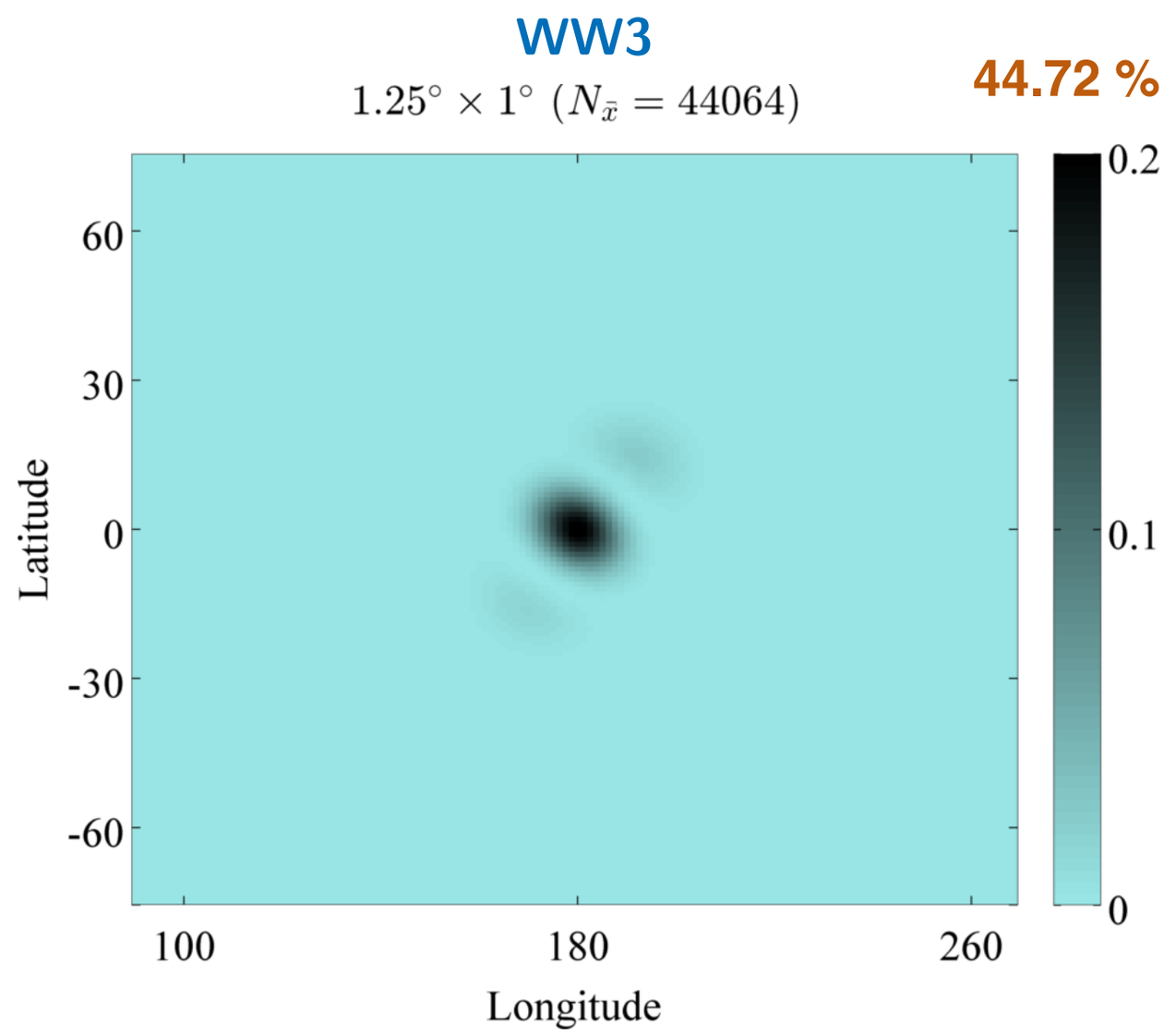

Figure: Relative total ℓ_2^2 errors after 1/2 revolution for different WW3 grid resolutions.

RBF-FD-W versus WAVEWATCH III

Relative total ℓ_2^2 errors over all directions

RBF-FD-W **4.24 %**

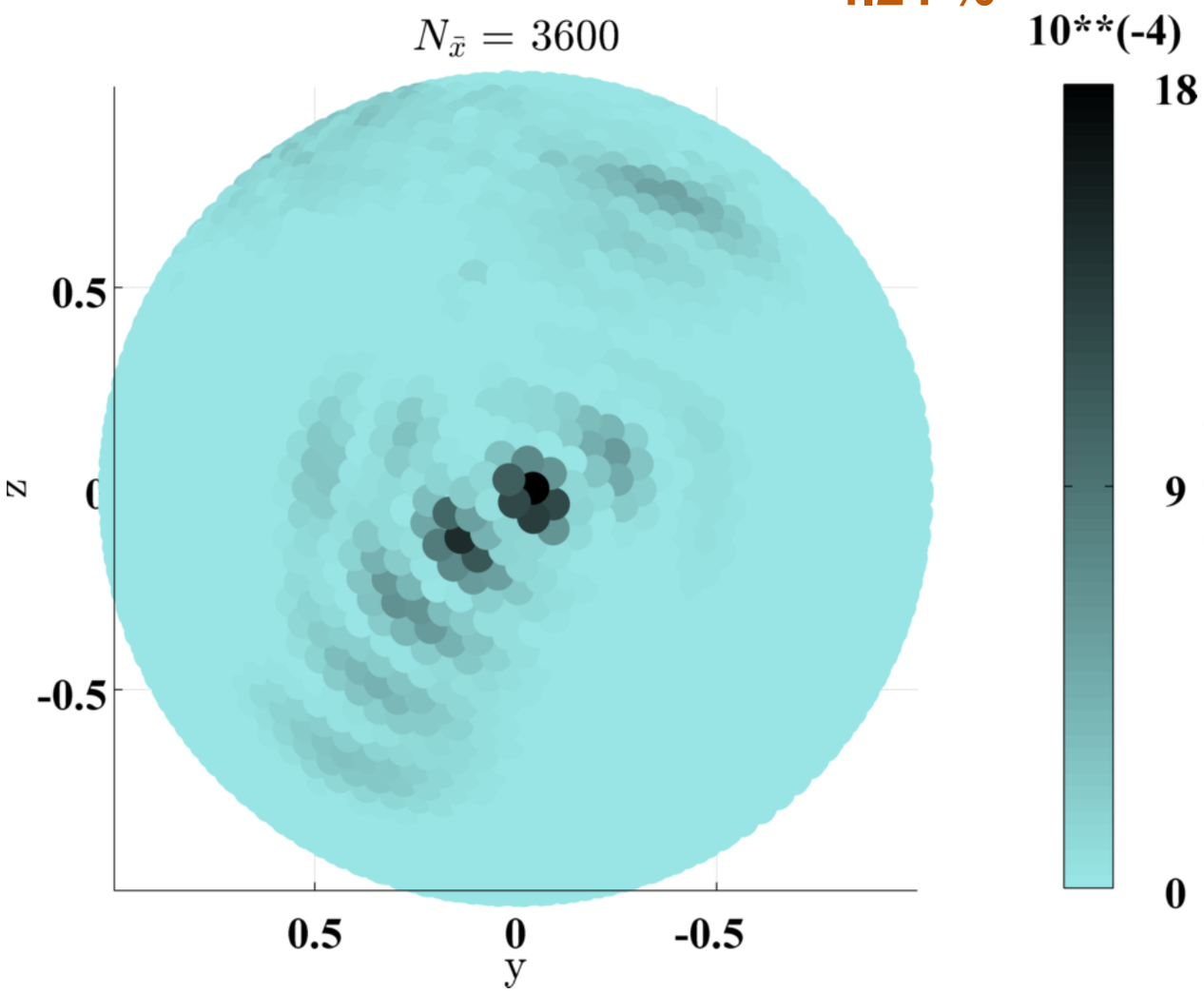

WW3 **44.72 %**

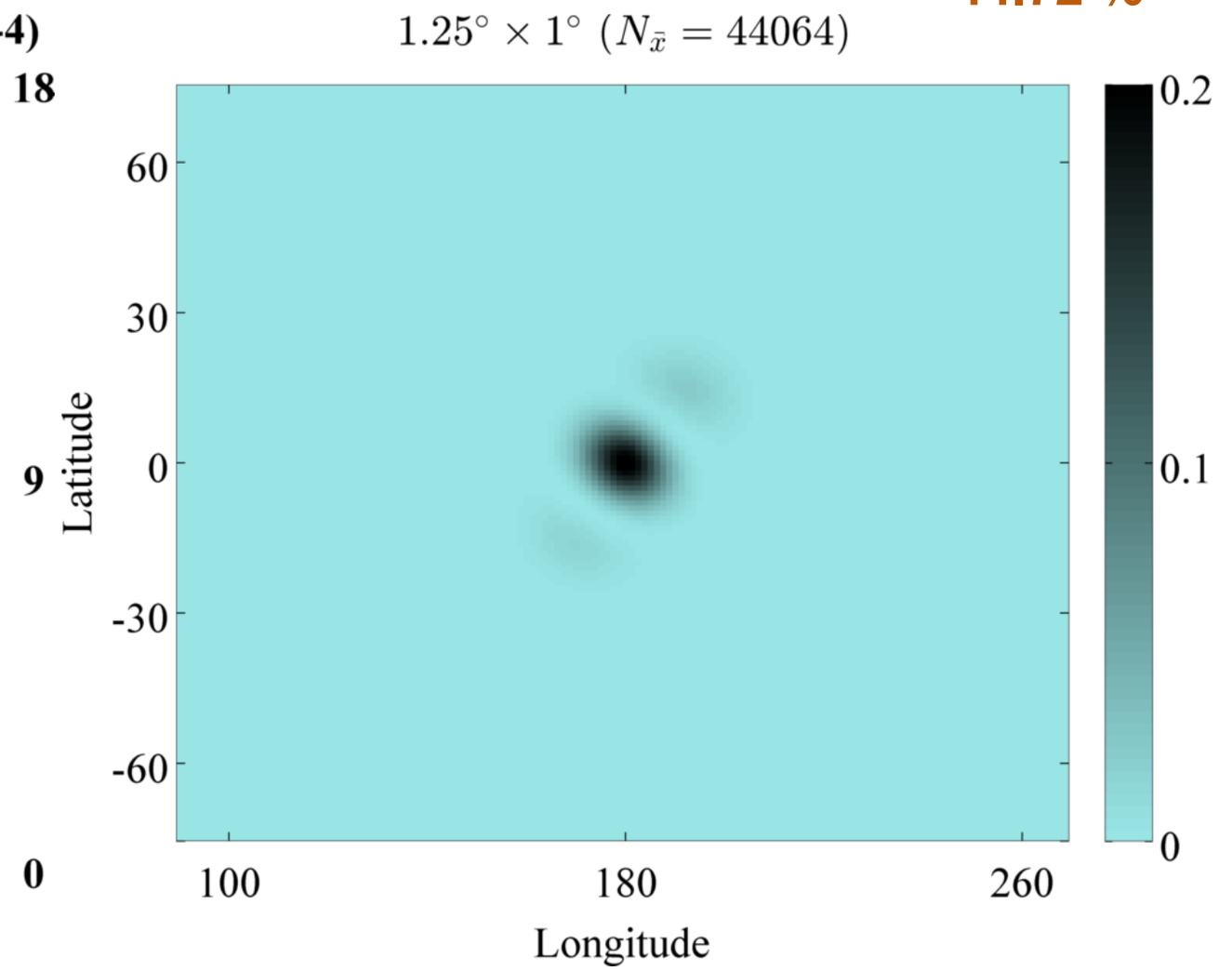

Figure: Comparison of relative total ℓ_2^2 errors after 1/2 revolution between RBF-FD-WAVE and WW3.

Outline

1. Scientific background
2. Coupled wave component
3. Overview of meshless approach
4. Kinematic prototype
5. Discussion

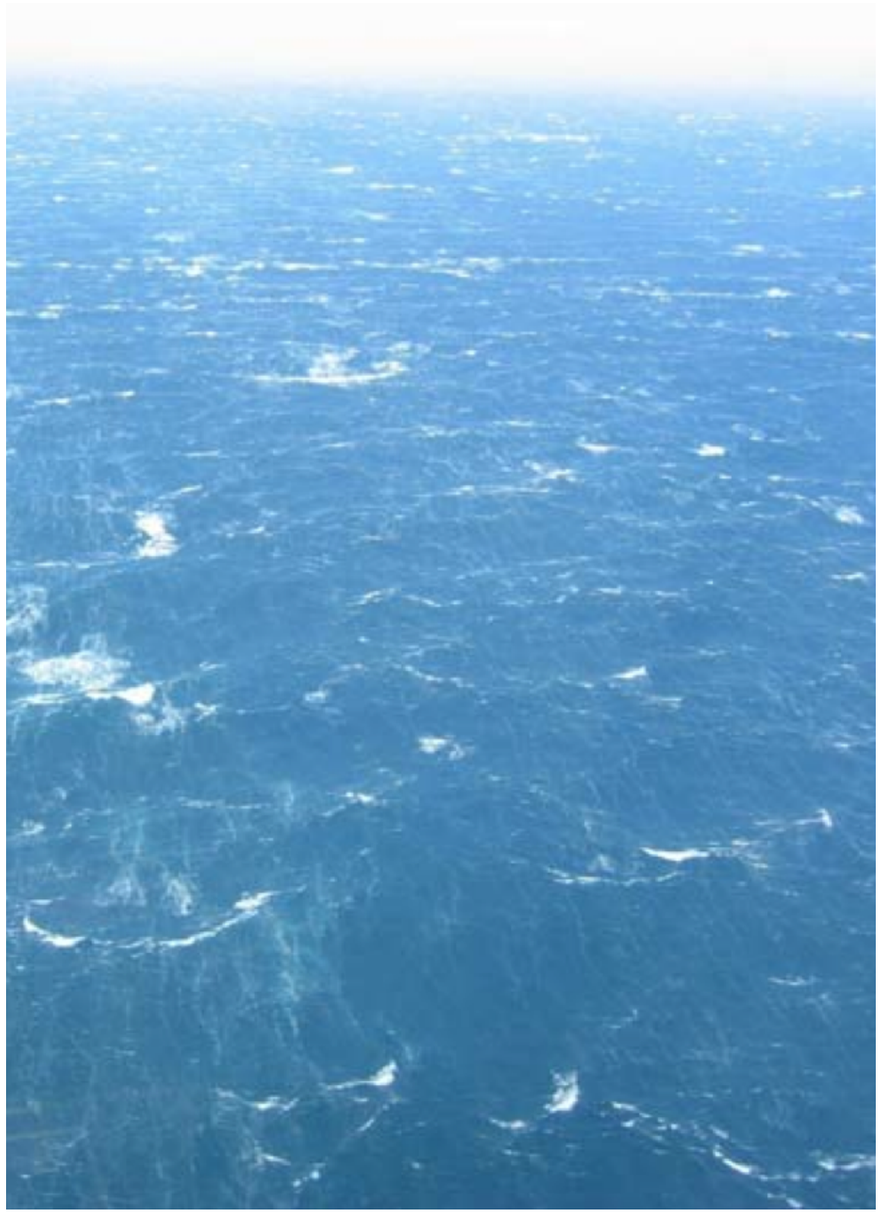

Wave action balance equation

The *wave action balance equation* can be derived on a coupled slab ($\vec{x}, \vec{k} \in \mathbb{R}^2$) from the *governing linear wave equations* and is given by

Spectral transport

$$\partial_t \mathcal{W} + \nabla_{\vec{k}} \Omega \cdot \nabla_{\vec{x}} \mathcal{W} - \nabla_{\vec{x}} \Omega \cdot \nabla_{\vec{k}} \mathcal{W} = \text{Sources}$$

Spectral changes

where

- $\sigma(\vec{x}, \vec{k}) = \left\{ g|\vec{k}| \tanh\left[|\vec{k}| H(\vec{x})\right] \right\}^{1/2}$ is the *intermediate-water dispersion relation*
- $\Omega(\vec{x}, \vec{k}) = \vec{U}(\vec{x}) \cdot \vec{k} + \sigma(\vec{x}, \vec{k})$ is the *Doppler-shifted dispersion relation*
- $\mathcal{W}(\vec{x}, \vec{k}, t) = \mathrm{g}\, \mathcal{S}_{\vec{k}}(\vec{k}; \vec{x}, t) \,/\, \sigma(\vec{x}, \vec{k})$ is the *spectral adiabatic invariant*
- "Sources" encompass the non-kinematic physics of the waves (generation, dissipation, nonlinear interactions, etc.)

Spatial refinement

Spectral

Spatial

Spatial

Width = 60 deg

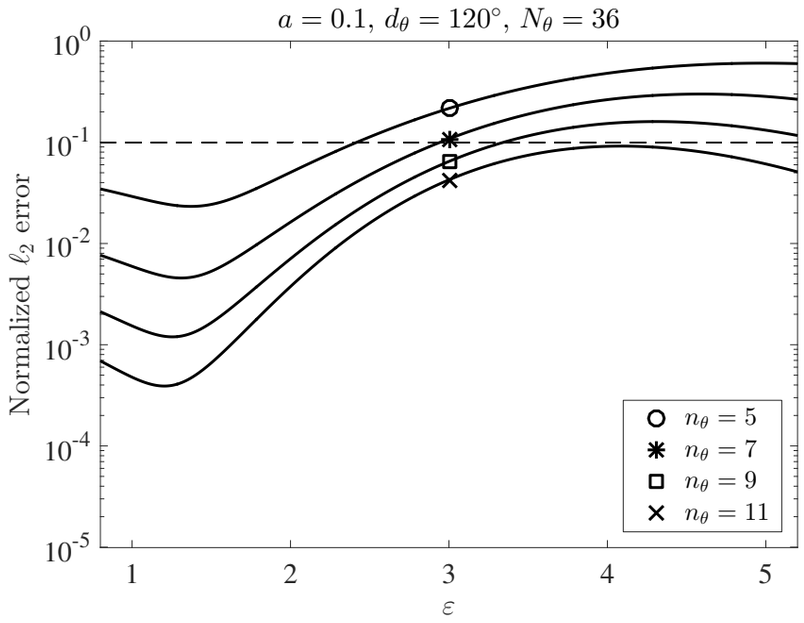

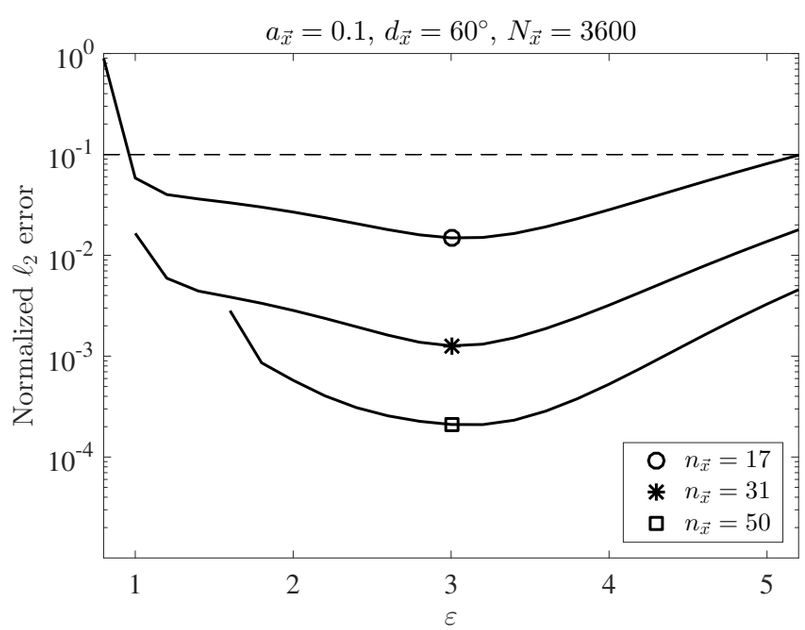

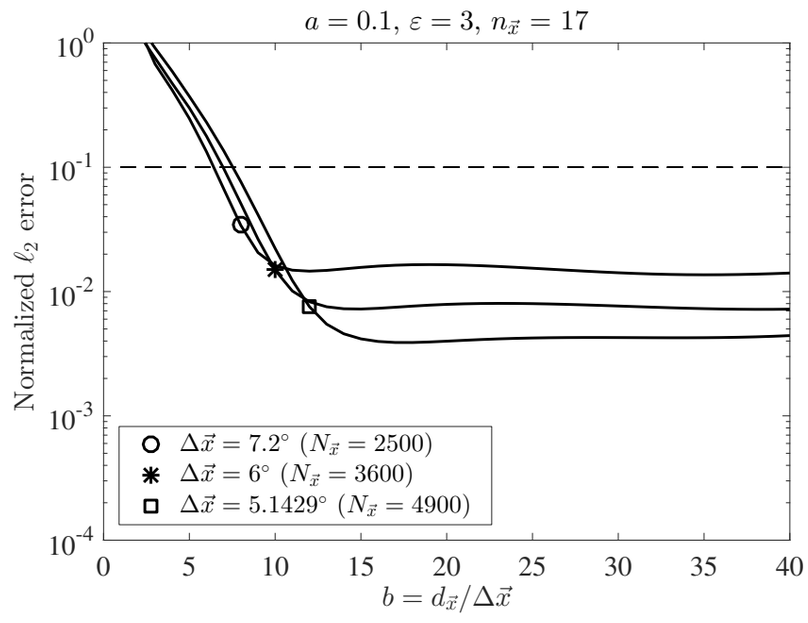

Width = 30 deg

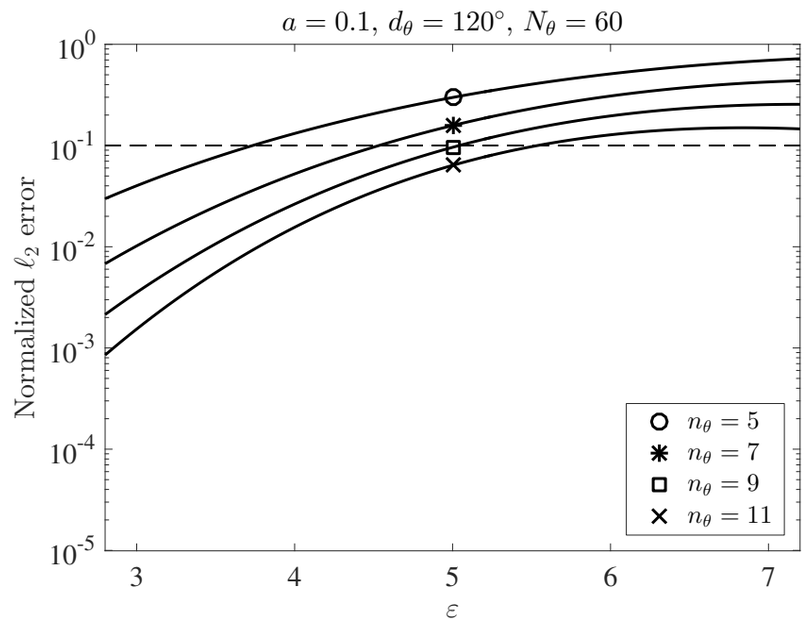

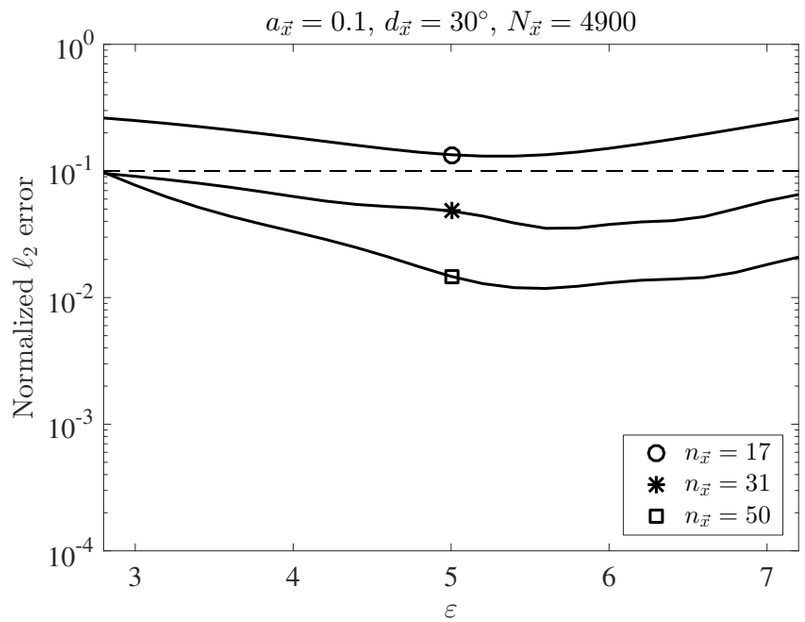

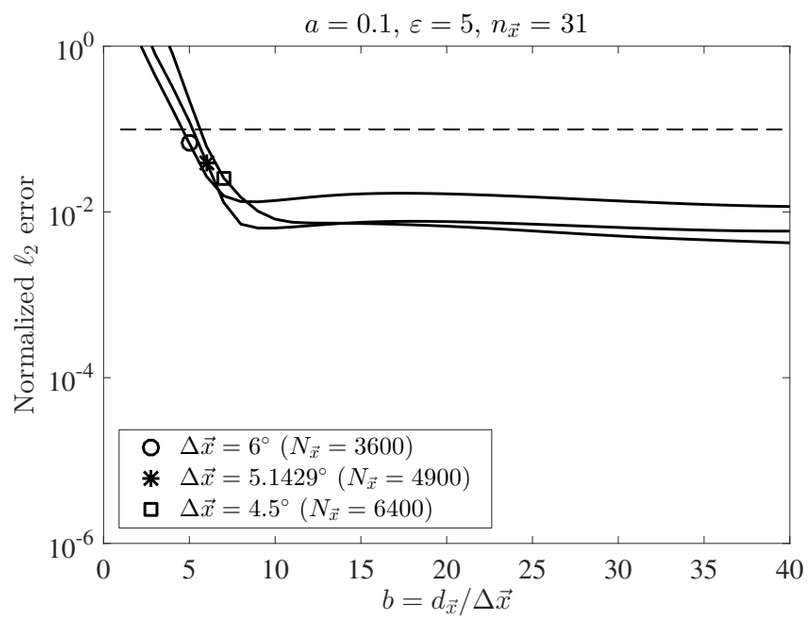

Figure: Comparison of current and potential spatial refinement tuning.

Next steps

Stage 2

- Replace current attenuation filter approach with physical boundaries

Stage 3

- Add source terms and wavenumber shifting (via time-splitting)

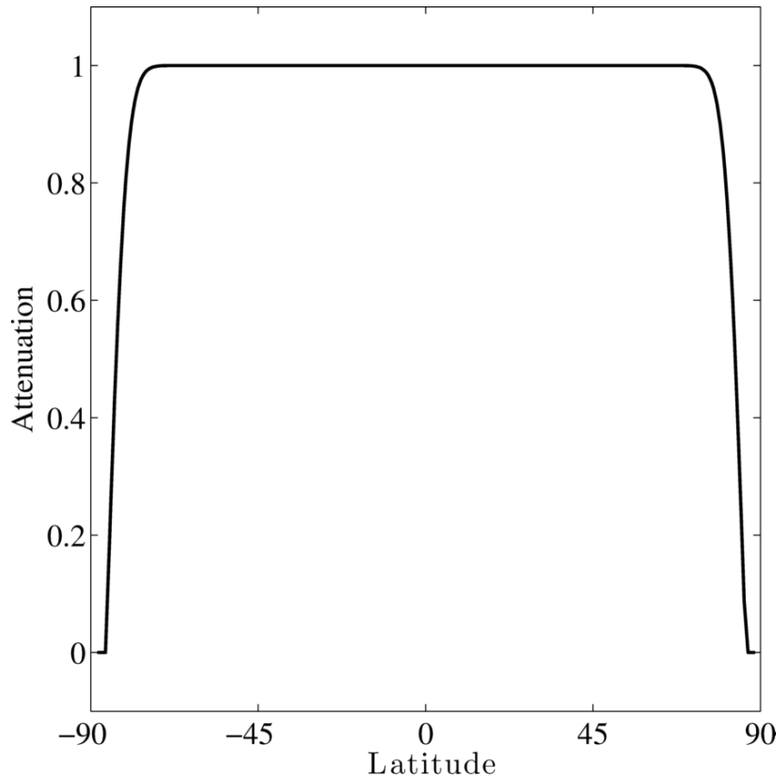

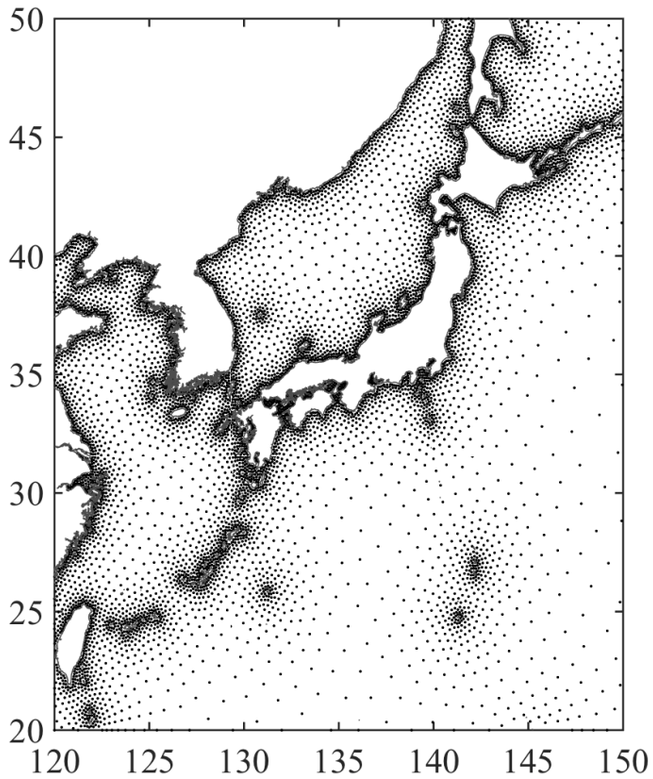

Figure: Examples of (a) boundary attenuation filter and (b) variable spatial node density.

Summary and conclusions

- WAVEWATCH III is now coupled to the NCAR Community Earth System Model ($3.2^\circ \times 4^\circ$ spatial, $25_f \times 24_\theta$ spectral grid)

- A meshless approach using RBF-FDs is a viable alternative for future spectral wave models (particularly for use in global climate model simulations)

- A monochromatic kinematic prototype performs well with limited computation (e.g., runs on a laptop)

- In simple tests the prototype compares well against higher resolution WAVEWATCH III runs:
  requires fewer unknowns ($\sim 1/12$) and is more accurate ($\sim 10\times$)

Thank You!

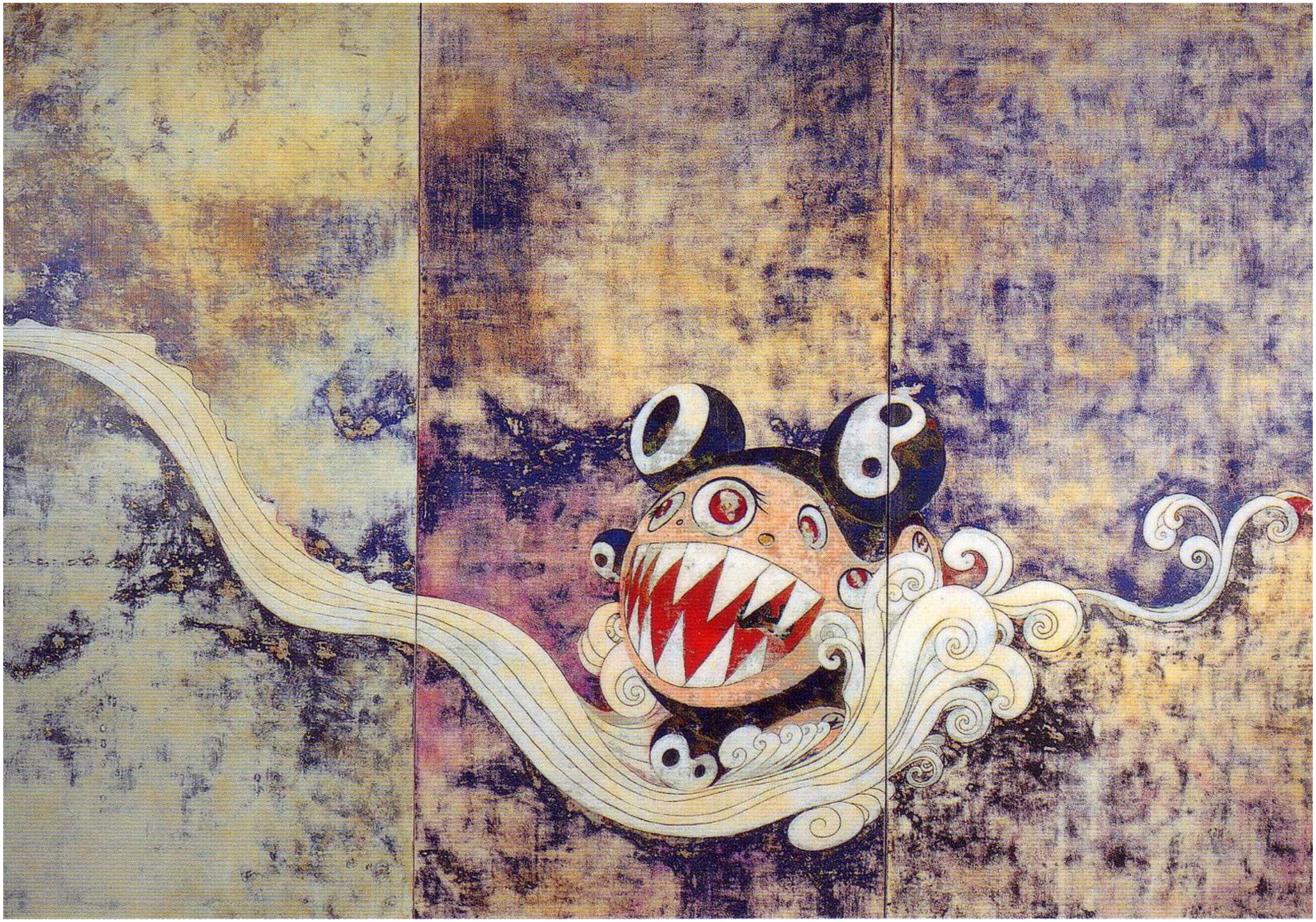

Figure: A modern reinterpretation of Hokusai's "The Great Wave" (Murakami, "727").